THE CASE FOR A CHRON 21 CHANGE IN AFRICA ABSOLUTE PLATE MOTION

A THESIS SUBMITTED TO THE GRADUATE DIVISION OF THE
UNIVERSITY OF HAWAIʻI AT MĀNOA IN PARTIAL
FULFILLMENT OF THE REQUIREMENTS FOR THE DEGREE OF

MASTER OF SCIENCE

IN

GEOLOGY AND GEOPHYSICS

MAY 2014

By

Sarah M. Maher

Thesis Committee:

Pål Wessel, Chairperson
Clinton P. Conrad
Richard Hey

Abstract

The India-Eurasia collision, a change in relative plate motion between Australia and Antarctica, and the coeval ages of the Hawaiian Emperor Bend (HEB) and Louisville Bend of ~chron 22–21 all provide convincing evidence of a global tectonic plate reorganization at chron 21. Yet if it were a truly global event, then there should be a contemporaneous change in Africa absolute plate motion (APM) reflected by physical evidence somewhere on the African plate. This evidence might be visible in the Réunion-Mascarene bend, which exhibits many HEB-like features such as a large angular change close to ~chron 21. Recently, the Réunion hotspot trail has been interpreted as a sequence of continental fragments with incidental hotspot volcanism. Here I propose the alternative hypothesis that the northern portion of the chain between Saya de Malha and the Seychelles (Mascarene Plateau) formed as the Réunion hotspot was situated on the Carlsberg Ridge, contemporaneously forming the Chagos-Laccadive Ridge on the India plate. I have created a 4-stage model that explores how a simple APM model fitting the Mascarene Plateau can also satisfy the age progressions and geometry of other hotspot trails on the African plate. This type of model could explain the apparent bifurcation of the Tristan hotspot chain, the age reversals seen along the Walvis Ridge and the diffuse nature of the St. Helena chain. To test this hypothesis we made a new African APM model that goes back to ~80 Ma using a modified version of the Hybrid Polygonal Finite Rotation Method. This method involves using seamount chains and their associated hotspots as geometric constraints for the model, and seamount age dates to determine its motion through time. The positions of the hotspots can be moved to get the best fit for the model and to explore the possibility that the chron 21 bend in the Réunion-Mascarene chain reflects African plate motion. I will examine how well this model can predict the key features reflecting African plate motion and contrast its predictions with other proposed models.

Table of Contents

i Abstract i

ii List of Tables iii

iii List of Figures iv

1 Introduction 1

2 Hotspot Chains on the African plate 3

2.1 Tristan-Walvis 4

2.2 St. Helena 5

2.3 Canary 5

2.4 Réunion 6

2.5 Other hotspot chains not used for modeling 7

3 Previous Models 9

4 Key Features and a Preliminary Stage Model 13

4.1 Stage A: Present to 20/30? Ma (~chron 6) 14

4.2 Stage B: 20/30 to 50 Ma (~chron 6–21) 14

4.3 Stage C: 50 to 67 Ma (~chron 21–30) 15

4.4 Stage D: 67 to 80 Ma (~chron 30–33) 15

5 Data 16

5.1 Geometric data 16

5.2 Age data 16

6 Methods 17

7 Discussion 19

7.1 Comparison to previous models 19

7.2 A chron 21 event along the Chagos-Laccadive Ridge 21

7.3 Model limitations 21

7.4 Implications for global plate motion 22

7.5 Outlook 23

8 Conclusions 24

9 References 49

List of Tables

1 Abbreviations for hotspot chains.....25
2 Age dated samples used for model constraints.....26
3 List of hotspot locations.....29
4 Absolute plate motion of Africa with uncertainties.....30

List of Figures

1 Hotspot chains on the African plate....32
2 Hotspots in the southwest quadrant of the African plate....33
3 Previous models for the Tristan hotspot....34
4 Previous models for the St. Helena hotspot....35
5 Hotspots in the northwest quadrant of the African plate....36
6 Previous models for the Canary hotspot....37
7 Hotspots on the eastern side of the African plate....38
8 Previous models for the Réunion hotspot trail....39
9 Stage A model....40
10 Magnetic anomaly picks between Africa and Antarctica....41
11 Stage B model....42
12 Stage C model....43
13 Stage D model....44
14 Residual topography of seamount chains....45
15 Revised Africa APM model....46
16 Africa APM predictions on the Chagos-Laccadive Ridge....47
17 Finite and stage reconstruction poles of the revised APM model....48

1. Introduction

Africa plays a key role in global plate reconstructions because of its stability over time, being surrounded by long-lived, divergent plate boundaries. These boundaries produce seafloor whose fabric and magnetic anomalies reflect clear relative plate motions with respect to neighboring plates. The continent traverses very slowly over the mantle, and over the past 100 Ma it has only moved between 500 and 900 km (Torsvik et al., 2008). The eastern margin of Africa began rifting from the Gondwana supercontinent in the early Jurassic period (~180 Ma), after volcanism along the Karoo Rift ceased. In the early mid-Jurassic (~160 Ma) spreading between Antarctica and Madagascar created the East Africa margin. Rifting between Africa and South America originated at the southernmost part of the continents at ~190 Ma and propagated northward. Seafloor spreading was initiated along the Mid-Atlantic Ridge, forming the Atlantic Ocean (eg., Seton et al., 2012). More recent episodes of spreading include the rifting between the Seychelles microcontinent and Madagascar by the start of chron 27n (61.98 Ma) and the formation of the Mascarene Basin via seafloor spreading (Collier et al., 2008). There is some debate over what time the fossil ridge in the Mascarene Basin went extinct, identifying the youngest seafloor age at chron 27n (Collier et al., 2008), or 68 Ma in the northern portion of the basin and 59 Ma in the south due to a southward propagating ridge extinction (Bernard and Munschy, 2000). Ongoing relative motion between the Nubia and Somalia plates over the past 11 Ma has resulted in ~100 km of motion (Royer et al., 2006). In general, relative motions between Africa and its neighbors are well understood, and all of the major tectonic plates, except for those in the Pacific Basin, can be linked via rifting or seafloor spreading going back to 200 Ma (Seton et al., 2012).

Since many plate reconstruction models use Africa as an anchor plate, its absolute plate motion (APM) needs to be known with high accuracy. The APM of a plate reveals how it moved over time relative to a fixed point in the mantle reference frame, usually defined by a set of hotspots. APM models use hotspots as either fixed or moving points to determine how the plate has moved relative to the mantle, utilizing volcanic chains on the plate as physical evidence for its past motion. In a fixed hotspot framework, the plate travels over a set of stationary hotspots so the impinging mantle plumes cause relatively

focused surface volcanism, creating volcanic chains that display linear age progressions. By fitting the geometry and age progressions of at least two hotspot chains on the plate, its motion over time is found. Recent models can also accommodate an amount of hotspot motion as predicted by mantle flow models while simultaneously fitting the geometry and age progression of volcanic chains (eg., Doubrovine et al., 2012; O'Neill et al., 2005).

There is growing evidence for a tectonic plate reorganization on a global scale around 50 Ma (Morra et al., 2013), or more likely closer to chron 21 (47.9 Ma). This time period includes the Australian-Antarctic plate reorganization (Whittaker et al., 2007; Whittaker et al., 2013) and the dramatic slowdown of the India plate (Copley et al., 2010). In the Pacific region this tectonic activity is concurrent with the South Pacific triple-junction reorganization (Cande et al., 1982) and formation of the Farallon-Pacific fracture zone bends (Caress et al., 1988), but the most intriguing evidence might be found within the Hawaiian Emperor Bend (HEB), which has been timed around 48 Ma (eg., O'Connor et al., 2013; Sharp and Clague, 2006). This 120° bend in the volcanic chain is believed to indicate a significant, 60° change in Pacific plate motion as it passed over the Hawaiian hotspot. However, this interpretation is not without controversy. Paleomagnetic evidence from the Emperor seamounts has indicated the plume could have drifted 10 to 15 degrees south (Tarduno et al., 2003), and if so the HEB would be a product of hotspot motion, not a change in the Pacific APM. However, coeval samples from the Hawaii and Louisville chains show no significant change in hotspot separation for the past 55 Ma (Wessel and Kroenke, 2009), and recent age dates from the Louisville bend also place it around the time of the HEB (Koppers et al., 2012). Furthermore, the interaction of the Hawaii plume with the nearby Kula-Pacific Ridge might have caused the surface volcanism to be produced closer to the ridge instead of directly over the plume head (Wessel and Kroenke, 2009). This gives credence to the idea that the HEB is a strong indicator of Pacific absolute plate motion change, even if it is affected by plume motion.

Curiously, the APM of Africa represented by previous models do not show a major change in motion around chron 21. The plate has less distinct hotspot trails and a slower movement over time when compared with the Pacific plate, making its motion much harder to detect. Yet, there are numerous indicators that a change in African plate

motion occurred around chron 21, as evidenced by the change in plate motions of both North and South America relative to Africa (Müller et al., 1999) and the fracture zone bends observed between Africa and Antarctica (Cande et al., 2010). It is thus possible that the APM of Africa remains incompletely understood.

Several differing models of Africa APM have been proposed, but no single model can fully explain the features observed on the plate itself, and none predict a major change in plate motion at chron 21. Apart from the overwhelming evidence from relative plate motion (RPM) studies, the geometry of key hotspot chains provide significant evidence for changes in absolute plate motion, including the inverted "C"-shaped curve of the Canary chain with a recent bend initiated around 20 Ma. More importantly, if the ridge-centered Réunion hotspot created both the Mascarene Plateau and Chagos-Laccadive Ridge simultaneously, it could have potentially formed the ~115° observed bend in the Réunion-Mascarene chain, which may be the equivalent of the HEB on the African plate. This bend could therefore reflect a chron 21 change in the APM of Africa, adding credence to the idea of a global plate reorganization at that time. A complimentary ~145° bend is also observed on the Chagos-Laccadive Ridge, which could show evidence for a chron 21 event on the India plate.

In this paper, I will explore key observational features on the African plate that need to be explained by any APM model, and test if a major chron 21 APM change could be a tectonic possibility for this plate. If so, this is likely to be reflected in the Réunion-Mascarene bend. Following a review of past models and a preliminary exploration of required stages of motion and the tectonic implications of these stages, I present available data and proceed to model the hotspot trails of four key hotspots on the African plate using a modified version of the hybrid Polygonal Finite Rotation Method (PFRM) (Wessel and Kroenke, 2008). This method will create a model for Africa APM whose predictions should fit the Réunion-Mascarene bend and simultaneously yield realistic results in the entire Indo-Atlantic region.

2. Hotspot Chains on the African plate

Burke and Wilson (1976) identified 43 hotspots on the African plate, 8 of which are in the ocean and an additional 10 are located close to ocean ridges (Figure 1). More recently, Courtillot (2003), using several criteria to diagnose a potentially deep mantle origin, settled on just three African plate hotspots. In their view, the major candidates were Afar, Réunion, and Tristan with "honorable mention" for the Canary and Cape Verde chains. While the continental Afar hotspot has not produced a suitable trail for modeling, I will discuss the others and several additional volcanic provinces on the African plate. I will demonstrate that these hotspots show evidence of being plume-related and could offer critical constraints on a new Africa APM.

2.1 Tristan–Walvis

Tristan-Walvis (Figure 2) is the longest-lived hotspot chain on the African plate, originating between 129 and 133 Ma (eg., O'Connor and Duncan, 1990; O'Neill et al., 2005); its hotspot is believed to be located near the Tristan da Cunha Island. As it was overrun by the Mid-Atlantic Ridge it formed two hotspot trails: the Rio Grande Rise on the South America plate and the Tristan chain on the African plate. Two apparently distinct trails, the Gough Lineament and the Walvis Ridge, were formed as parts of the Tristan-Walvis chain. There are several hypotheses for how these trails have formed, including the presence of two hotspots (O'Connor and Duncan, 1990) or spatial zonation of the hotspot plume (Deppe et al., 2010). The hotspot pair explanation is unlikely because of the close proximity of these segments, and the spatial zonation explanation is a case of special pleading for the Tristan chain, which lessens the arguments for a plume origin (Anderson, 2001). Consequently, current models of Africa APM have not addressed this bifurcation, typically choosing instead to follow the northern lineament along the Walvis Ridge (Figure 3). Age dating along the Walvis Ridge has revealed age reversals of more than 10 Ma between seamounts in relatively close proximity where a linearly increasing age progression would be expected. Newly redated samples (Rohde et al., 2013) have failed to rectify this problem. This anomaly might be explained by uncertainties in the ages themselves, sampling biases in between dredge sites,

simultaneous volcanism in different areas along the chain, or a large diameter plume conduit (O'Neill et al., 2005). Alternatively, it could be an indication of an aspect of Africa APM not presently understood or modeled.

2.2 St. Helena

Approximately 2000 km north of the Tristan chain lies the St. Helena hotspot chain (Figure 4), which displays a linear age progression from the present day to 80 Ma. Any older seamounts would have been overprinted by more recent Cameroon Line volcanism (Figure 4). Courtillot et al. (2003) described St. Helena as a non-primary hotspot with no lower mantle origin, unrelated to plume volcanism. The chain itself is very dispersive with a diffuse trail up to 500 km wide in some locations and is characterized by low-amplitude seafloor volcanic features. This confused expression could be due to the presence of through-cutting fracture zones acting as zones of weakness and allowing for a broader zone of hotspot volcanism (O'Connor and Le Roex, 1992). Most of the dated seamounts are concentrated at the young end of the chain, presenting uncertainties in the details of age progression for the older section. Despite Courtillot et al.'s (2003) assessment, we choose to include it in the modeling in order to provide broad coverage of hotspots on the plate.

2.3 Canary

The Canary chain (Figure 6), found to the northwest of the African continent, has a distinctive inverted "C" shape, presumably due to its close position to the Euler poles describing Africa APM. It appears to have originated at ~67 Ma, though the influence of the plume has been detected geochemically within the Madeira-Tore Rise going back to the Cretaceous (Geldmacher et al., 2006). Models of African APM often fail to accurately recreate this shape, leading to alternative non-hotspot explanations for this mismatch, such as intraplate deformation (Steinberger et al., 2004) or edge driven convection cells interacting with the Canary plume (Geldmacher et al., 2005). There is also an abundance of rejuvenated volcanism, with Tenerife, La Palma, and el Hierro islands all experiencing volcanic activity within the past 100 years. While this may be expected given a slow

APM and hence close proximity of the hotspot to its associated features, it makes the onset of hotspot volcanism at points along the chain very difficult to determine.

2.4 Réunion

The Réunion hotspot trail (Figure 7) started with the arrival of the plume head in the Deccan Traps at ~67 Ma, forming the Chagos-Laccadive Ridge on the India plate before it was overrun by the Carlsberg Ridge and producing volcanism on the African plate as well (Duncan and Richards, 1991). Previous models generally predict the hotspot first to have formed the Saya de Malha Bank, then the Nazareth and Caragados Carajos Banks further south and finally the Mauritius and Réunion Islands (Figure 7). There is some controversy over a submarine plateau, referred to in this paper as the Mascarene Plateau, which extends to the northwest from the Saya de Malha Bank to connect with the Seychelles microcontinent. Three seismic profiles along the ridge have indicated flat lying sedimentary beds which are potentially limestone in nature (Bunce and Chase, 1966), and it has been recently proposed that the plateau, Chagos-Laccadive Ridge, the Saya de Malha Bank, Nazareth Bank, and Mauritius are actually continental fragments (Torsvik et al., 2013). Alternatively, a drill site along the Mascarene Plateau found massive basalt basement rocks from the early Paleocene (Backman et al., 1988), and a potentially small magnetic anomaly was found, causing the hypothesis to be posed that it was a more deeply buried portion of the volcanic ridge to the south (Bunce and Chase, 1966). Seismic refraction on Saya de Malha indicated a crustal composition intermediate between continent and ocean, with the base displaying a seismic velocity close to that of Pacific volcanic islands (Fisher et al., 1967). Volcanic activity on the Seychelles had a hotspot origin, and the reconstructed volcanic region lay nearly radially above the plume generation zone during the eruption of the Deccan Traps (Ganerød et al., 2011), so it is not unreasonable to suspect that the Mascarene Plateau could partly have been formed by hotspot volcanism. Additionally, it is unknown how long the Réunion hotspot was centered below or near the Carlsberg Ridge, during which time the Mascarene Plateau could have developed contemporaneously with the Chagos-Laccadive Ridge. There is limited age data along the Réunion hotspot track, which has made pinpointing the exact hotspot position at chron 21 difficult. The region is also complicated by seafloor

spreading in the Mascarene Basin, which terminated with the extinction of the Mascarene Ridge within a few Myr of the onset of the Réunion hotspot (Bernard and Munschy, 2000). While the timing is similar, it appears that the seafloor on which the Réunion hotspot produced its volcanic edifices was fixed to the rest of the Somalia plate when the volcanism occurred. Additionally, more recent but limited motion between Nubia and Somalia would have introduced some motion bias on the order of 100 km (Royer et al., 2006).

2.5 Other hotspot chains not used for modeling

Several other hotspot chains are present on the African plate but were not used to constrain the fit for the new hotspot model, for various reasons (i.e., lacking ages, being relatively short-lived, etc.). I will instead use these trails for model validation purposes. These chains are detailed below.

The Cape Verde hotspot chain (Figure 5) is a more recent hotspot but its oldest volcanism is not well constrained. The earliest date was reported as 26 Ma on Sal using K-Ar dating techniques, though current Ar/Ar dating has given Sal an age of ~17 Ma, and the most recent volcanism in the chain was 0.3 Ma ago (Holm et al., 2008). Episodic volcanism is common among all the islands within this chain and can last for several Ma. Its close proximity to the African plate Euler poles means very little motion is expected, and this may be reflected in the observed overprinting, making the onset of volcanism difficult to determine. The presence of a significant swell suggests it is caused by a mantle plume (McNutt, 1988).

The Bathymetrists seamount chain (Figure 5) in the Equatorial Atlantic has a general southwest to northeast trend off the Sierra Leone coast of Africa. Zircon dates of ~58 Ma from the Carter seamount at the older end of the chain reveal that the volcanic chain probably formed in the early Eocene (Skolotnev et al., 2010). While it does have a distinct track compatible with plate motion predictions, no Ar/Ar ages have been taken along the chain so the lifespan of the hotspot cannot be established.

The New England hotspot has been quite prolific in the formation of seamount chains, first creating the White Mountains and Corner Seamount chains on the North American plate, then the Great Meteor chain on the African plate (Figure 5). The most

recent volcanism has been on the Great Meteor seamount with an age of 17.32 Ma (Geldmacher et al., 2006). No other ages have been measured in the Great Meteor chain to the north, though recurrent volcanism has been observed. Several of the seamounts could have formed simultaneously (Tucholke and Smoot, 1990), so the geometry of the chain would not be a reliable constraint on the fit of my model.

The Madeira hotspot chain (Figure 5) is just to the north of the Canary hotspot chain and crosses the Azores-Gibraltar Fracture Zone onto the Eurasia plate. It has been extensively sampled for age dates. Younger (mid- Miocene – Pleistocene) volcanism is superimposed on a much older (Late Cretaceous) basement most likely related to the Canary hotspot (Geldmacher et al., 2006). However, the proximity of the Africa-Eurasia plate boundary contributes to weak lithospheric zones and tectonic deformation that could affect the location and orientation of volcanism (Geldmacher et al., 2005), obscuring the true hotspot trail. The Canary chain shows a much clearer age progression and orientation, and its close proximity to the Madeira chain means the latter would exhibit a similar hotspot track and add minimal new information to constrain the final model.

The Shona, Discovery, and Bouvet hotspots are all located to the south of the Tristan chain near the Mid Atlantic Ridge. Recent age samples from Shona and Discovery chains (Figure 2) indicate the hotspots initiated only ~44−41 Myr ago and have a northeast age-progressive trend (O'Connor et al., 2012). While these hotspot trails show the general trend of the African plate after 40 Ma, they do not add new constraints on the parameters of my plate motion model. The nearby Bouvet hotspot trail has been difficult to resolve due to the influence of the Southwest Indian Ridge and Shaka Ridge (Figure 1). Without age dates along the ridge and a distinct trail the geometry cannot be separated from nearby formations (O'Connor et al., 2012).

The Marion hotspot trail originated on southeast Madagascar at ~90 Ma (Torsvik et al., 1998), with a vague trace winding southward along the Madagascar plateau to a ridge shaped bathymetry anomaly slightly north of the Southwest Indian Ridge (SWIR). Then, the trace crosses the SWIR to the Antarctica plate before reaching Marion Island (Duncan and Richards, 1991). However, its current location on another plate means that

RPMs would have to be taken into account to fit the unclear and undated hotspot trail on Africa, making it an unreasonable choice to fit in my modeling.

The Crozet hotspot is presently located under the Antarctic plate, 750 km away from the southwest Indian Ridge. Its trail consists of 5 islands and islets composing the Crozet Archipelago and an underlying basaltic plateau dated at 54 Ma. The Crozet bank supporting the archipelago is considered the current position of the hotspot plume, with volcanism going back to the SWIR in the early Eocene (Breton et al., 2013). Crozet's position on the Antarctic plate and the lack of Ar/Ar age dates make it too problematic to incorporate in the fit of the model.

The Comores hotspot chain (Figure 7) lies to the north of Madagascar and is composed of the Comores Islands and potentially extending back through the Farquhar and Armirante atolls before terminating at the Seychelles microcontinent. K/Ar age dates of the Comores Islands reveal an increasing age moving eastward, but the more recent northwest trend of the hotspot trail is inconsistent with all current models. Instead this orientation is attributed to the relative plate motions between Nubia and Somalia over the past 10 Ma (Emerick and Duncan, 1982). Its deviating trend means it is unlikely to reflect motion of another hotspot in such close proximity to Réunion, hence another tectonic explanation is more likely; I therefore chose not to include this chain in my modeling.

Finally, the Cameroon Line (Figure 5) is a volcanic trail that originates in continental Africa, with its youngest features potentially overwriting the oldest portion of the St. Helena hotspot trail. Recent studies indicate that the source of volcanism is due to lithospheric instabilities caused by top-down cooling (Milelli et al., 2012). The lack of age progression along the trail and recurrent volcanism along its entire continental length makes a hotspot origin unlikely, so the trail was not used for modeling.

3. Previous Models

The first APM model for Africa was created by Morgan (1981) in which the plate was positioned over a hotspot reference frame defined by the Canary, Tristan, Crozet, Réunion, and Kerguelen hotspots. All hotspots appeared to be stationary within 5 degrees, and much of the scatter was assumed to be due to errors in the plate motion

reconstructions incorporated into the model. Morgan predicted that better models of seafloor spreading would see some of that scatter eventually disappear (Morgan, 1981).

O’Connor and Duncan (1990) expanded on the Africa APM model by using ages along Walvis Ridge of the Tristan hotspot chain. They extrapolated the hotspot trails by assuming that hotspots are fixed relative to one another and the basement ages and geometry of the Walvis Ridge accurately represent the APM. It also predicted that the Réunion hotspot followed the trend from Réunion Island to the Saya de Malha Bank between 0 and 36 Ma, but moved more slowly than expected based on the age dates. This discrepancy could be due to motion between the Réunion and Tristan hotspots or RPM occurring in the African Rift Zone (O'Connor and Duncan, 1990).

Radiometric ages and the geometries of the Walvis Ridge and the Cameroon Line were key observations constraining the Duncan and Richards (1991) APM model. Their model then predicted the age progression and geometry of the Mascarene Ridge in the Réunion trail and the Madagascar Ridge of the Crozet hotspot trail. The agreement between the predicted and observed hotspot trails gave credence to the idea that hotspots move very slowly in the Indo-Atlantic reference frame, concluding that hotspots have remained fixed for the past 60 Ma. There was also excellent agreement along the Réunion hotspot trail if the hotspot was centered at a seamount to the west of Réunion Island (Duncan and Richards, 1991).

O’Connor and Le Roex (1992) incorporated the Gough Chain and Walvis Ridge from the Tristan hotspot trail along with the St. Helena and Réunion hotspots to revise the Africa APM model. The predicted Tristan hotspot trail followed a more northerly route than its predecessors, and the APM exhibited a slower plate velocity from 40 Ma to present day and between 120–80 Ma than previous models, though it does not fit the St. Helena hotspot chain particularly well. The predicted age distribution along the Réunion chain was significantly different from the recorded ages, which could be due to the location of the hotspot used (O'Connor and Le Roex, 1992), or that a fossil spreading axis under Réunion created a different route for plume melt (Bonneville et al., 1988).

In a major improvement, Müller et al. (1993) constrained a new APM model by incorporating 11 hotspot trails from Africa and several of its neighboring plates. Hotspot track segments were considered simultaneously by using the relative plate motions for a

particular age range. In this way, ages and geometry for the Chagos-Laccadive Ridge were incorporated into the Réunion hotspot track. The study concluded that there was no major motion between the Indo-Atlantic hotspots going back 84 Ma (Müller et al., 1993).

The hypothesis of moving hotspots was proposed to explain several inconsistencies that had resulted when using a fixed hotspot reference frame, including the inability to explain anomalous paleolatitudes in the Emperor seamount chain (Tarduno et al., 2003) and the inability to reconcile the Atlantic and Pacific hotspot reference frames (Molnar and Stock, 1987). O'Neill et al. (2005) were the first to incorporate moving hotspots into an Africa APM model, modeling the motion back to 120 Ma. Dynamic simulations of plume motion were created and constrained using plate kinematics, tomography and sparse paleomagnetic data. Whenever there was an observed age reversal along the Tristan chain the oldest reliable age was used. The preferred moving hotspot model yielded reasonable motions and broadly satisfied the available paleolatitude and geochronology data. However, predictions from moving and fixed hotspot reference frames were not significantly different above their uncertainties since 80 Ma, but required larger hotspot motions (5˚–10˚) for times prior to 80 Ma (O'Neill et al., 2005).

Cande and Stegman (2011) recently created an Africa APM by summing the APM of Antarctica (Müller et al., 1993) and a new relative plate motion model describing motion between Africa and Antarctica (Cande et al., 2010). Their APM predicted a better fit to the Great Meteor and Tristan hotspot chains than that of the Müller et al. (1993) model, but showed little difference in the Réunion hotspot track (Cande and Stegman, 2011).

A new moving hotspot global model was created by Doubrovine et al. (2012) using five hotspots believed to be sourced by plumes from the lower mantle in the Atlantic (Tristan-Walvis and New England), Pacific (Hawaii and Louisville) and Indian (Réunion) oceans. Plume motion was determined by numerical modeling of whole mantle convection combined with the advection of plumes into the mantle flow field. The resulting framework of moving hotspot locations was then used to create a global APM model going back to 80 Ma (Doubrovine et al., 2012). The predicted hotspot track for Réunion was examined in detail by Torsvik et al. (2013), who analyzed zircons found on

the island of Mauritius and proposed that several key features of the Réunion hotspot track were actually continental fragments from Madagascar and India. For the past 50 Ma the Réunion hotspot trail has then coincidentally followed the fragments along the Mascarene Plateau. If these features are indeed continental, then any APM model based on this hotspot trail would necessarily be suspect (Torsvik et al., 2013).

Several complications with the current models need to be addressed. Rifting between the Nubia and Somalia plates (Royer et al., 2006) may have moved positions up to ~100 km, and the development of the Mascarene Basin during 68-59 Ma (Bernard and Munschy, 2000) may have caused minor relative plate motion between the Réunion trail on the Somalia plate and the rest of the Africa hotspot trails (on the Nubia plate). On-axis hotspot volcanism can affect the geometry of the hotspot chains, including Tristan, Réunion, and the Madeiras, thus biasing any modeling attempts. Lithospheric striations could potentially increase seamount chain dispersion, particularly along the St. Helena track (O'Connor and Le Roex, 1992). The distribution of seamount ages can also be obscured by dredging techniques, which typically collect the younger material on the outer surface of the seamount, making the actual date of onset volcanism difficult to determine for such a slow moving plate (O'Connor and Le Roex, 1992). In terms of constraining hotspot motion, the only available paleolatitude data are from the Tristan and Réunion chains. The latter has a predicted northern motion of 8 mm/yr (Vandamme and Courtillot, 1990), while Tristan has a 4–7 degree anomaly (Sager and Tominaga, 2008) or 10 degrees of southward motion from 130–80 Ma followed by relatively no movement (Hall and Bird, 2007). In general, the slow-moving nature of the plate and limited and unreliable sampling of seamounts has made the motion of the African plate much less constrained when compared with APM models for the Pacific plate. By using the Hybrid Polygonal Finite Rotation Method (Wessel et al., 2006) I will obtain the geometric model and time constraints independently from each other, improving on the geometries of previous Africa APM models.

4. Key Features and a Preliminary Stage Model

There are several physical indicators on the African plate that reveal more or less abrupt changes in plate motion at specific times. The APM models generally attempt to replicate this behavior, but for any specific time period one particular model might do a better job than another. The Duncan and Richards (1991) and Müller et al. (1993) models produce similar predictions for the hotspot trails, though they differ in the length of time represented by the Réunion track and choice of hotspot locations. Both mimic the north-south trend of the Canary chain and its east-west trend for more recent times, but not to the degree represented in the chain itself. The O'Neill et al. (2005) moving hotspot model also shows the trend of the Réunion track up to the Nazareth Bank, but further north there is a sharp excursion to the west into the Mascarene Basin that is not supported by any observed features. Their model also suffers at early times (~10 Ma) from an apparent increase in hotspot motion, so the predicted hotspot tracks abruptly change direction away from their currently prescribed hotspot positions. The Doubrovine et al. (2012) model was fit using only the Réunion and Tristan hotspot chains from the African plate, but predictions for other plume motions were also published, allowing me to examine the APM model predictions for these additional chains as well. While there is a reasonable fit to the Réunion chain, the predicted Tristan hotspot trail trends to the south around 70 Ma instead of following the observed trend to the north, and there is an extremely poor fit to the Canary chain. The general trend of the St. Helena hotspot is predicted, though its trail is placed much further east than in previous models. All of the APM models discussed show a general trend of Africa moving northeast over time, but there are several key features formed on the African plate during four time intervals that I suggest reasonable APM models should broadly replicate. Thus, my proposed model seeks to reproduce what I see as key indicators of plate motion change for these time intervals. To highlight these features I have created an approximate 4-stage model to explore what the implications are for the entire plate when these features are satisfactorily modeled, and to guide the actual modeling.

4.1 Stage A: Present to 20/30? Ma (~chron 6)

Inferred volcanic propagation rates along the St. Helena chain suggest that the plate is moving ~33% slower since at least 19 Ma (O'Connor et al., 1999), which coincided with an increase in continental volcanism at ~25 Ma (Burke and Wilson, 1972). This change appears to correlate with the observed bend in the Canary chain near Fuerteventura, dated around 20 Ma (O'Connor et al., 1999). However, sparse dating along the St. Helena track allows for other interpretations that indicate the African plate could have begun slowing down between ~30 Ma or even ~40 Ma (O'Connor et al., 2012). There is, however, no clear identifiable geometric change along the St. Helena chain, and any subtle signal would be hard to infer due to the diffuse nature of the chain. Therefore, from 0–20 Ma (stage A), the key objective was to match the youngest trend of the Canary chain and the southern portion of the Réunion chain as closely as possible while simultaneously honoring the age progressions and geometries of the other chains. This was accomplished by creating a best fit line from the current hotspot position to a point along the chain approximately dated at 20 Ma for the Réunion and Canary chains. Bisectors for both lines were produced, and the pole for this stage rotation is located at the intersection of the two bisectors. These conditions imply an Euler pole close to the Canary chain (Figure 9-a), which results in a satisfactory fit to all the chains (Figures 9b and c).

4.2 Stage B: 20/30 to 50 Ma (~chron 6–21)

There are signs that a change in African plate motion occurred around chron 21, as evidenced by the change in plate motions of both North and South America relative to Africa (Müller et al., 1999) and the fracture zone bends observed between Africa and Antarctica (Cande et al., 2010), which I have interpreted as a consequence of a major Africa APM change expressed by the Réunion-Mascarene bend (Figure 10). From 20-50 Ma, Stage B replicates the trend of the Réunion hotspot chain up to the Saya de Malha Bank while simultaneously predicting a Canary hotspot trail with a more north-south orientation. Using the same method as stage A, the bisectors of the best fit lines for the Canary and Réunion chains from 20–50 Ma were found, and their crossing indicated the

location of the stage pole. These conditions produce a stage rotation that has good agreement among the other hotspot chains (Figure 11).

4.3 Stage C: 50 to 67 Ma (~chron 21–30)

Fracture zone bends between Africa and Antarctica reflect a substantial change in relative plate motion at chron 30 (Cande et al., 2010) which coincides with the onset of Réunion hotspot volcanism in the Deccan Traps (Chenet et al., 2007) and the termination of the Réunion-Mascarene trail at the Seychelles microcontinent, respectively. This time interval corresponds to the formation of the Mascarene Plateau. A median line was constructed through the plateau and a single-stage rotation pole was assumed to be located somewhere along its bisector. Stage C was modeled using two different approaches, both assuming that a stationary Réunion hotspot produced the Mascarene plateau during this time interval. If the rotation pole along the bisector is located slightly east of the Tristan chain, then reversals in several Atlantic hotspot trails would be predicted (Figure 12a). However, if it is located to the west of the chain, then no reversal but a sideways jog would be predicted (Figure 12b). A reversal in the hotspot trail has interesting implications along the Tristan chain because it could potentially explain some of the age reversals that have been observed along the Walvis Ridge at the time, as well as the puzzling bifurcation of the chain itself.

4.4 Stage D: 67 to 80 Ma (~chron 30–33)

The northern trend of the Walvis Ridge around 80 Ma is the earliest recorded change in Africa APM reflected in the hotspot chains, indicating a change in the location of the Euler pole (O'Connor and Le Roex, 1992). The hotspot trail of the only other long-lived hotspot chain, St. Helena, is obscured by Cameroon Line volcanism, so plate motion past this time frame would have to incorporate hotspot trails from neighboring plates using relative plate motions (eg., Müller et al., 1993); this is beyond the scope of this thesis. Stage D is thus a continuation of the model from 67 to 80 Ma by fitting the St. Helena and Tristan chains only, as no other chains are older than ~70 Ma (Figure 13).

Armed with this first-order assumption I will model the Africa APM using the hybrid Polygon Finite Rotation Method of Wessel et al. (2006). First, I review the data sets used in this endeavor.

5. Data

5.1 Geometric data

Initially, the topography of the hotspot chains on the African plate must be isolated from other features in the ETOPO2 global relief grid. The background seafloor elevation was removed using a spatial median filter. At a given location, the median elevation within a 700 km diameter circle was found and subtracted from its elevation. To remove anomalies that were less pronounced in height, such as mid-ocean ridges and fracture zone tracks, an elevation cutoff of 700 meters was applied. Thus, bathymetric features with a background seafloor corrected height below 700 m were not considered to be part of the hotspot chain. Other features that were not caused by hotspot volcanism were removed manually by enclosing each hotspot chain in a polygonal envelope. Any feature outside the envelope is not considered part of the volcanic hotspot chain. This partitioning allows continental features within a chain (eg., the Seychelles), volcanism that does not describe the geometry of the main hotspot path (eg., Rodrigues Ridge, Selvagem Islands), or features associated with fracture zones (eg., those crossing the St. Helena chain) to be removed in order to clarify the hotspot trail signals.

The residual grid for the Réunion chain region required an extra component due to its contemporaneous formation with the Chagos-Laccadive chain. As the Carlsberg Ridge crossed the Réunion hotspot, a significant portion of the volcanic chain near the Réunion bend rifted off to form part of the Chagos-Laccadive Ridge on the India plate, leaving a corresponding piece missing on the African plate between the Saya de Malha and Nazareth Banks. In order to create a more realistic fit to the hotspot chain, this portion of the Chagos was isolated and rotated back to its location at ~42.5 Ma using the Africa-India rotation model (Müller et al., 2008) to fill in the observed gap. The resulting residual topography for each chain can be seen in Figure 14.

5.2 Age data

Whenever possible, $^{40}Ar/^{39}Ar$ isochron ages were used for the model constraints because they are typically more robust. Isochron ages were selected if the $^{40}Ar/^{36}Ar$ ratio was greater than or equal to 295.5 within its given uncertainties, and $^{40}Ar/^{39}Ar$ plateau ages were used if the ratio was below that value. Because of the sparse age data across Africa, some K/Ar ages were also incorporated into the model in the Canary chain. A lack of samples along the Réunion chain also motivated an age from the Chagos-Laccadive Ridge to be rotated onto the Réunion chain using the same method as was explained above for the missing piece in the residual topography (Table 2). Sample locations are shown in Figure 1.

6. Methods

The method for determining my new Africa APM model closely follows the hybrid Polygonal Finite Rotation Method (PFRM) described in (Wessel et al., 2006), with a few modifications to account for circumstances that are unique to the African plate motion. With residual topography of the hotspot chains specified, their associated hotspot positions are used to determine all compatible rotations. Given the limited evidence for hotspot motion and the finding of O'Neill et al. (2005) that hotspot motion proved insignificant after 80 Ma for this preliminary work, I have used a set of fixed hotspot locations (Table 3). I expect that any systematic mismatch between my model and the data is likely to reflect this assumption. A given opening angle is tested over a full range of rotation pole locations. Each rotation that reconstructs the hotspot on or within a given distance threshold of its associated chain is considered a "hit" and recorded, with preference given to rotations that fit a higher number of chains simultaneously. When all of the hits are accumulated, quaternion filtering is used to find the smoothed rotation poles as a function of rotation angle, yielding an ideal geometric model.

Dated seamounts on the African plate were used to determine how the plate moved in time. Their positions can be associated with an opening angle using the geometric model, forming an age-angle relationship. Then, any age (and its uncertainty) can be interpolated for a given angle in the geometric model, yielding the final APM

model. While the hybrid PFRM yields reasonable results in the Pacific plate (Wessel et al., 2006; Wessel and Kroenke, 2008), systematic problems in how the method averages opening angles had to be addressed when it was applied to modeling African plate motion.

Initial results revealed rotations that successfully reconstructed the Mascarene Plateau onto the Réunion hotspot, but once all rotations were averaged the resulting geometric model would not predict a trail overlaying that part of the chain, veering off toward the east instead. The rotations resulting in hits along the Mascarene Plateau actually represented a very limited range of opening angles not differing by more than one degree or less. Instead, I found that the rotation pole locations were moving while the rotation angle remained nearly constant. The hybrid PFRM uses opening angle as a proxy for age, so the method breaks down when the angle is not monotonically increasing along the hotspot trail. Consequently, the smoothing of rotations as a function of angle ended up averaging all these different pole locations, yielding a single, meaningless rotation. Hence, increasing angle could not be used as a proxy for age for this section, and a new proxy had to be found. In the simplest terms, increasing distance from the hotspot indicates older hotspot material, so distance along the Réunion trail was explored as a preliminary proxy for age.

In order to test my hypothesis, I wanted to focus on the rotations that yielded acceptable results along the Réunion hotspot chain. In order to filter these rotations as a function of distance, a median line was determined through the entirety of the chain. At 50 km intervals along this line, a circle of 100 km radius was positioned and used to find all reconstructed points ("hits") that fell within that radius. The rotations associated with these reconstructed points were then filtered to find the average rotation pole and angle for each circle. This yielded a set of rotations that fit the entirety of the Réunion hotspot chain up the Mascarene Plateau while honoring the other chains included in the modeling. This set of rotations predicts reversals along several hotspot chains on the western side of Africa similar to my exploratory stage model (Figure 12a), and in contrast to the alternate model (Figure 12b) where no reversals are present.

Another obstacle was the sparse ages on the African plate and reconstruction angles that were not monotonically increasing along the chain, contributing to an

unreliable age-angle relationship. A hotspot trail age grid map was interpolated from the known ages which allowed me to produce the expected age for a given position along any hotspot chain in order to compensate for the sparse age data along each trail. Separate grids were made for seamount and island ages and their interpolated uncertainties. Then the age-distance relationship was used to determine the APM model up to the terminus of the Réunion chain at ~65 Ma. With only the St. Helena and Tristan chain used for further analysis beyond 67 Ma, the APM obtained from the PFRM was appended to extend the model back to ~80 Ma (Figure 15).

7. Discussion

7.1 Comparison to previous models

Morgan (1981) only specified hotspot locations for the Madeira, Great Meteor, and Discovery chains. My estimates based on his figures and the best fit to his model allowed me to compute predictions for other hotspot trails. The Morgan APM yields similar hotspot trails as my new APM model, especially in early time periods from 0–30 Ma, but a significant difference is that the plate motion his model predicts is much smaller, meaning a slower African plate. Morgan (1981) predicted a Réunion trail that only goes as far back as the Nazareth Bank before terminating at 68 Ma, which does not agree well with my present age estimates of ~45 Ma. Additionally, the Morgan estimate of Cape Verde being active from 120–70 Ma is very different from current age estimates of the hotspot.

O'Connor and Duncan (1990) made a prediction based on just the Tristan hotspot and O'Connor and LeRoex (1992) developed another model based on both the Tristan and St. Helena hotspots. For the time period from 0 to 80 Ma my model matches the general trend of both of the hotspot paths predicted by these APM models, though the reversal is not represented in either of their models. The location my model predicts for chron 21 is slightly further up the chains. Both of their models followed the northern portion of the Tristan chain without following the southern Gough lineament.

The Duncan and Richards (1991) model does not seem able to replicate the St. Helena and Tristan hotspot tracks with much accuracy, but that is most likely due to my

estimates of their hotspot positions; the trend of the trails is otherwise similar. Their fit to the Cape Verde hotspot is better than my revised model, but fitting it has created artifacts along the Canary hotspot trail, creating a sharp bend when no bend is present. This means my model more smoothly replicates these trails, and follows the Canary shape more accurately. Their model also indicates a departure from the Réunion hotspot trail at the northern end of the Nazareth Bank at 36 Ma.

There are many similarities between my new APM and the Müller et al. (1993) model, particularly in the Réunion, St. Helena, and Tristan hotspot tracks. The Müller model does not predict the presence of seamounts in the northern part of the St. Helena chain and only follows the northern portion of the Tristan chain. My new APM predicts a much closer fit to the Canary hotspot chain, but it fails to follow the Great Meteor hotspot trail, where the Müller et al. (1993) model follows the path more closely. However, due to ridge interaction and a lack of age dates along the trail, it is not a conclusive test.

Initially, the O'Neill et al. (2005) predicted hotspot track shows many similarities to my new Africa APM though it is less smoothly rendered and suggests bends along the Tristan chain where there are none, including a southern-sweeping trend from 0–20 Ma to fit the Gough lineament. This is most likely due to the predicted motion of the Tristan hotspot from their mantle model during that time period. The Réunion track flows back to the Saya de Malha bank at ~40 Ma, though the trend cuts into the Mascarene Basin where no volcanic features are seen. It is then projected on to the Chagos-Laccadive Ridge. On the St. Helena track, the hotspot trend is very similar until the 67–80 Ma mark, where it follows a more southern route through the seamount chain. The O'Neill et al. (2005) trend along the Great Meteor trail follows the residual topography of the chain closely.

While the model of Cande and Stegman (2011) does an excellent job of fitting most of the 4 stages, it fails when it comes to recreating the Canary bend. This underestimate of the bend is also reflected in the early stages of the Tristan chain, where it has taken a more southern route. At later stages it does fit both the St. Helena and Tristan chain, though the hotspot trail trends to the center of the Tristan chain and ignores the bulk of seamounts on the northern lineament from chron 5r (10.4 Ma) to chron 18r (42.7 Ma).

The Doubrovine et al. (2012) model does not replicate what I see to be many of the key features on the African plate. From 0–30 Ma, the predicted Canary trail trends in

the opposite direction of its actual geometry, and the geometry of the hotspot trail along the Tristan and St. Helena hotspot chains suffers at later ages, moving away from the observed trail. Their predicted Réunion trail is a reasonable fit up to the Saya de Malha bank, where it is then projected to move on to the Chagos-Laccadive Ridge. However their trail is predicted to be on the western side of the Réunion track rather than the middle, which is attributed to it being continental in origin. In general my model better predicts the observed hotspot trail.

7.2 A chron 21 event along the Chagos-Laccadive Ridge

An interesting consequence of the new APM occurs on the Chagos-Laccadive Ridge on the India plate (Figure 16). Previous models have predicted the Réunion hotspot forming the ridge from 60 to ~40 Ma, then crossing the Carlsberg Ridge to the African plate. When my model predictions are reconstructed on the India plate using India-Africa relative plate motions, a reasonable fit to the ridge is produced, though it appears to be offset to the east (Figure 16). This is a systematic error suggesting that other factors, such as mantle flow or the unmodeled Nubia-Somalia motion, might be at work. When the projected hotspot trail is adjusted 200 km to the east, it closely follows the residual bathymetry hotspot trail and reveals the presence of a ~50 Ma event in the Chagos-Laccadive trail evidenced as a slight bend (~145°) between the Chagos Ridge in the south and Laccadive Ridge in the north. Basalts from the ODP-713 drill site close to that bend have an age of 49.6 Ma, which could indicate that this bend is the global chron 21 event as recorded in India APM. Early motion on the Vishnu Fracture Zone could have erased the prominence of this feature on its eastern side. My model replicates the presence of the bend and follows the trail more closely than previous model tracks.

7.3 Model limitations

Many of the model limitations come from determinations of what physical indicators on the African plate are truly attributed to plate motion. In particular hotspot or mantle motion, recent Nubia-Somalia plate motion, and Paleocene seafloor spreading in the Mascarene Basin could have contributed to systematic errors in the model determination. What many previous models associate with a hotspot motion, I associate

with a change in plate motion because the coherent motions of many African hotspots support this, and the limited amount of paleomagnetic data on the African plate does not fully constrain either possibility. Plate motion between Nubia and Somalia over the past 11 Ma would also bias the inferred rotations and may lead to errors of up to 100 km in the predictions of the Réunion and Chagos-Laccadive trails. The age of the seafloor in the Mascarene Basin is also very close to the timing of the onset of Réunion volcanism on the African plate at ~67 Ma. If the basin continued to spread it might cause systematic errors in estimates of rotations that include the Mascarene Ridge and possibly obscure any event around chron 21.

The Carlsberg Ridge also poses a problem for the exact positioning of the Réunion hotspot. Conjugate magnetic anomalies around the ridge are progressively wider in separation, which is inconsistent with rotations that fit the Indian, Capricorn and Somali plates at times earlier than chron 22o (Cande et al., 2010), so the location of the Carlsberg Ridge is not well constrained for those time periods. The amount of time it spent over the Réunion hotspot is not known, and interactions between the plume and the ridge could have caused surface volcanism to form closer to the ridge axis instead of directly above the hotspot (Wessel and Kroenke, 2009). If the Réunion hotspot was not situated below the Carlsberg Ridge from 67 Ma to chron 21, then it could not have concurrently formed the Mascarene Plateau and the Chagos-Laccadive Ridge.

7.4 Implications for global plate motion

Comparing my African plate motion with previous models is most intriguing for the ~45–65 Ma interval. The African plate appears to stop its northeastward motion during the arrival of the Réunion plume head at the Deccan Traps at 67 Ma (Chenet et al., 2007). This corresponds with the inferred slowdown or pivoting of the African plate proposed by Cande and Stegman (2011). This change in absolute plate motion could also corroborate their idea of the Réunion plume push forcing Africa's change in motion. During that time period, the African plate appears to pivot as the total reconstruction pole moves in a more northwestern direction and the stage poles cluster near the approximate stage C pole (Figure 17). The plate then resumes its general northeast motion around

chron 21, possibly following the collision of India into Eurasia around chron 20 (Cande et al., 2010) or other proposed explanations for the global reorganization.

Preliminary results suggest that the projection of my new Africa APM model via plate circuits into the Pacific fails to make an appreciable difference in the prediction at the HEB, which could have many explanations. For instance, this could indicate a breakdown in the plate circuit between Africa and the Pacific plate if RPMs are not known with a high accuracy. The plate circuit I used was Africa – West Antarctica – East Antarctica – Pacific (Seton et al., 2012). Antarctic plate motions are not well resolved, particularly between East and West Antarctica. The HEB not being reproduced might be due to that uncertainty, and further research would be necessary to determine if Antarctic RPMs also reflect a chron 21 event. Additionally, the African plate moves so slowly relative to the mantle that even a notable change in plate motion might not lead to significant changes in the global plate circuit. It is noteworthy that a large APM change along the Réunion trail projects to a gentle bend for the Chagos-Laccadive Ridge on the India plate, so a significant bend in the Pacific regime might not be expected.

7.5 Outlook

While this model offers a self-consistent explanation for many of the important features on the African plate, several of the hypotheses require verification. The most important data to examine these hypotheses further would be an increase in the quantity and quality of age dating along the Réunion-Mascarene trail. Volcanic evidence along the Mascarene plateau would add validity to my hypothesis that it has a hotspot origin, and any age dating along the chain would help to identify the precise location of the chron 21 event along the chain and improve my age-angle relationship. In general, an increase in the number of dated seamount chains will help to constrain my model parameters, and $^{40}Ar/^{39}Ar$ dating along previously undated chains would allow them to be used to verify some of my model's claims. This would be particularly interesting along the Bathymetrist chain, where my model predicts a hotspot trail reversal event similar to the one seen in the Tristan chain, so any age reversals that are observed would add validity to my model. Finally, better coverage of ages from both Tristan and St. Helena may be needed to confirm the age reversal predicted by my model.

My model could also be improved by accommodating an amount of hotspot motion, but I have refrained from doing so due to the relative lack of paleomagnetic data from all four plumes and the sparsity of age control. Although my model successfully matches the Réunion -Mascarene trail, the possible presence of continental fragments along part of the chain requires further investigations. It would also be beneficial to look at the impact of this revised APM model on the net rotation of the lithosphere.

8. Conclusions

- It is geometrically possible to include the Mascarene Plateau as the continuation of the Réunion hotspot track while honoring the geometries of other hotspot chains, giving credence to the idea of a chron 21 event being present in the APM of Africa.
- Africa APM projected into the India reference frame predicts a gentle bend in the Chagos-Laccadive Ridge at chron 21, as is observed in the topography.
- A reversal in the Tristan hotspot track might better explain its apparent bifurcation and the reversals in observed age progression along the Walvis Ridge.
- The St. Helena hotspot track reversal could explain why there is a higher concentration of seamounts in the northern portion of the chain.
- The Canary hotspot track can be projected back to the Madeiras, which agrees with isotopic evidence of a Canary plume influence as detailed in Geldmacher et al. (2006).
- The African plate appears to stop its northeastward motion during ~45-65 Ma, which corresponds with the inferred slowdown or pivoting of the African plate proposed by Cande and Stegman (2011).
- Africa APM projected via the global plate circuit into the Pacific does not predict the HEB.

Table 1. Abbreviations for hotspot chains.

Name	Abbreviation
Bathymetrist	BA
Chagos-Laccadive	CH
Canary	CN
Cape Verde	CV
Discovery	DI
Great Meteor	GM
Madeira	MA
Shona	SH
St. Helena	ST
Tristan	TR
Réunion	RE

Table 2. Age dated samples used for model constraints.

Sample	Lon (E°)	Lat (°N)	Age (Ma)	± (Ma)	Comments	Citations (Age, Location)
			Réunion			
Piton de Fournaise	55.71	-21.24	0	2	Active volcanism, oldest age on Réunion Island is K-Ar	1, Piton de Fournaise
Mauritius	57.47	-20.4	7.5	7.5	Isochron age	2, Piton de la Petite Riviere Noire
NB-1	60.3	-15.0	31.5	0.3	Isochron age	2, 3
SM-1	60.0	-9.5	47.5	3.6	Isochron age	2, 3
ODP 115-706	61.37	-13.11	32.9	0.7	Isochron age	2, 4
ODP 115-707	59.02	-7.55	64.1	1.1	Isochron age	2, 4
ODP 115-713	63.57	-11.64	49.6	.06	Rotated from Chagos-Laccadive Ridge using Müller et. al (2008) rotations	
			Chagos-Laccadive Ridge			
ODP 115-713	73.39	-4.19	49.6	0.6	Isochron age	2, 4
ODP 115-715	73.83	5.08	57.5	2.5	Isochron age	2, 4
			Tristan-Walvis			
CH19 DR3-2	9.33	-19.37	114.1	0.2	Plateau age, weighted mean	5, 5
CH19 DR3-22	9.33	-19.37	108.3	0.4	Plateau age, weighted mean	5, 5
CH19 DR4-1	9.02	-19.85	112.8	0.45	Plateau age	5, 5
CH19 DR4-2	9.02	-19.85	112.4	0.55	Plateau age	5, 5
CH19 DR4-3	9.02	-19.85	112.6	0.4	Plateau age	5, 5
DSDP Leg 74-525A-57-2	2.99	-29.07	71.3	0.4	Plateau age, weighted mean	5, 5
DSDP Leg 74-525A-57-5	2.99	-29.07	72.0	0.6	Plateau age	5, 5
DSDP Leg 74-528-43-2	2.32	-28.53	66.9	1.95	Plateau age	5, 5
AII-93-5-3	-5.03	-34.29	36.1	0.5	Plateau age	5, 5
AII-93-6-1	-4.98	-34.35	33.4	0.5	Plateau age	5, 5
AK-1695-6	-7.73	-36.42	27.0	0.05	Plateau age	5, 5
420-1-DR21-1	2.55	-32.79	47.0	0.1	Plateau age	5, 5
423-1-DR25-4	0.55	-34.93	45.6	0.05	Plateau age	5, 5
AII-93-10-11	-1.57	-34.34	49.4	0.35	Plateau age	5, 5
PS69/440-1-DR32-2	-2.43	-37.48	37.1	0.1	Plateau age	5, 5
PS69/440-1-DR32-5b	-2.43	-37.48	36.9	0.1	Plateau age	5, 5
AII-93-3-1	-7.78	-37.1	28.4	0.6	Isochron age	6, 6
AII-93-3-25	-7.78	-37.1	30.8	0.4	Isochron age	6, 6
AII-93-7-1	-3.63	-34.5	38	0.2	Isochron age	6, 6
AII-93-8-11	-3.48	-34.5	35.6	0.3	Isochron age	6, 6
AII-93-11-8	-0.02	-32.97	62	1.3	Isochron age	6, 6
V29-9-1	1.12	-32.63	50	7.1	Isochron age	6, 6
AII-93-14-1	2.39	-31.99	60.2	1	Isochron age	6, 6
AII-93-14-19	2.39	-31.99	59.9	2	Isochron age	6, 6

DSDP 74-528-40-5	2.32	-28.53	79.1	6.3	Isochron age	6, 6
AG51-2-1	-12.28	-37.12	0.64	0.3	Isochron age	7, 7
AG51-7-1	-8.55	-40.17	8.1	0.8	Isochron age	7, 7
AG51-9-1	-6.22	-39.47	18.7	0.2	Isochron age	7, 7
				St. Helena		
AC-D-02H	4.77	-2.32	80.2	0.4	Plateau age	7, 7
AC-D-05A	4.47	-4.28	77.5	0.4	Plateau age, 4 28'7" W used instead of E	7, 7
AC-D-06	1.55	-8.42	52.3	0.3	Plateau age	7, 7
AC-D-02E	4.77	-2.32	79	0.9	Isochron age	7, 7
AC-D-02B	4.77	-2.32	80.1	1.3	Isochron age	7, 7
SO84 43DS-1 (Kutzov)	-8.35	-15.14	10.3	0.3	Isochron age	8, 8
SO84 53DS-1 (Benjamin)	-8.52	-16.2	7.5	0.5	Isochron age	8, 8
SO84 60DS-2 (Josaphine)	-9.01	-16.27	2.6	0.3	Isochron age	8, 8
SO84 68DS-1 (Bonaparte)	-7.1	-15.6	15.3	1.1	Isochron age	8, 8
SO84 68DS-2 (Bonaparte)	-7.1	-15.6	15.1	0.03	Isochron age	8, 8
SO84 68DS-5 (Bonaparte)	-7.1	-15.6	14.9	0.1	Isochron age	8, 8
SO84 68DS-6 (Bonaparte)	-7.1	-15.6	14.2	0.6	Isochron age	8, 8
SO84 69DS-2 (Bonaparte)	-6.95	-15.8	14.5	0.5	Isochron age	8, 8
M16/1-6 (Bonaparte)	-7.01	-15.64	15.1	0.2	Isochron age	8, 8
SO84 71DS-6 (Bagration)	-6.56	-15.38	17.9	0.3	Isochron age	8, 8
SO84 72DS-2 (Bagration)	-6.49	-15.41	18	0.5	Isochron age	8, 8
SO84 73DS-1 (Bagration)	-6.47	-15.42	18.8	0.2	Isochron age	8, 8
SO84 74DS-1 (Bagration)	-6.46	-15.44	18.9	0.3	Isochron age	8, 8
				Canary		
DS 822-4 (Conception)	-12.66	29.82	16.8	1.4	Isochron age	9, 9
DS 822-2 (Conception)	-12.66	29.82	18.1	3.2	Isochron age	9, 9
Lars	-13.29	32.8	68.2	2	Isochron age	9, 9
Tenerife	-16.61	28.27	11.29	0.24	Isochron age, oldest reported age	10, Tenerife Island
Hierro	-18	27.75	1.12	0.02	K-Ar age, oldest reported age	11, Hierro Island
La Palma	-17.87	28.67	2	0.1	K-Ar age, oldest reported age	12, La Palma Island
Gomera	-17.13	28.1	15.5	1.3	K-Ar age, oldest reported age	13, Gomera Island
Gran Canaria	-15.6	27.97	14.64	0.29	K-Ar age, oldest reported age	14, Gran Canaria Island

Fuerteventura	-14.02	28.33	20.4	0.4	K-Ar age	15, Fuerteventura Island
Lanzarote	-13.63	29.04	15.5	0.3	K-Ar age	15, Lanzarote Island

References: 1, (McDougall, 1971); 2, (Duncan and Hargraves, 1990); 3, (Meyerhoff and Kamen-Kaye, 1981); 4, (Vandamme and Courtillot, 1990); 5, (Rohde et al., 2013); 6, (O'Connor and Duncan, 1990); 7, (O'Connor and Le Roex, 1992); 8, (O'Connor et al., 1999); 9, (Geldmacher et al., 2001); 10, (Thirlwall et al., 2000); 11, (Guillou et al., 1996); 12, (Ancochea et al., 1994); 13, (Cantagrel et al., 1984); 14, (Guillou et al., 2004); 15, (Coello et al., 1992)

Table 3. List of hotspot locations.

Name	Lon	Lat	Used for fit	Radius (km)	Start time (Ma)
Réunion	54.7	-21.5	Yes	70	67
Tristan	-12	-38.5	Yes	60	129
St. Helena	-8.5	-16	Yes	80	80
Canary	-17.25	28	Yes	60	67
Cape Verde	-25	15	No	75	26
Madeira	-17.3	32.6	No	75	76
Shona	0	-51.6	No	75	44
Discovery	-4.7	-45	No	75	44
Bathymetrist	-28	4	No	75	58
Great Meteor	-28.5	30	No	75	80

Table 4. Absolute plate motion of Africa with uncertainties. The angle is given in degrees, Ages are in Ma, and a–f given in rad^2. For the uncertainties k is set to 1 and g to 10^{-5}. Covariance estimates for the kth rotation are given by

$$c_k = cov(\boldsymbol{r}_k) = \frac{1}{\hat{k}_k}\begin{bmatrix} a_k & b_k & d_k \\ b_k & c_k & e_k \\ d_k & e_k & f_k \end{bmatrix} g_k$$

Lon	Lat	Age	Angle	a	b	c	d	e	f	DOF
-63.2	63.7	3.88	-0.64	5.07	1.44	3.45	-0.34	1.3	5.6	2898057
-53.2	66.95	4.15	-0.8	6.01	1.1	3.75	0.08	1.1	9.12	3645922
-47.49	69.01	4.35	-0.94	7.12	0.84	3.85	0.17	0.53	13.18	4269477
-38.28	68.82	4.68	-1.09	7.92	0.1	4.25	-0.68	-1.34	16.23	4487976
-35.73	69.87	5.24	-1.46	9.25	-0.22	6.65	-2.81	-3.98	17.08	3779436
-39.03	68.58	6.26	-1.94	11.15	0.78	11.35	-5.81	-7.22	17.99	2773938
-45.34	63.66	8.03	-2.53	13.43	4.67	18.07	-9.56	-13.94	24.45	1677395
-53.11	61.44	9.77	-3.24	16.8	8.84	25.84	-13.18	-21.41	29.39	1001073
-59.19	59.17	11.43	-3.91	19.3	11.75	28.74	-16.05	-24.16	32.2	666491
-61.08	56.99	12.93	-4.44	19.78	12.31	29.33	-15.91	-24.29	31.58	468853
-62.37	55.38	14.49	-4.99	18.6	11.4	29.72	-14.1	-24.45	30.44	340696
-63.69	54.07	16.28	-5.66	16.35	8.81	28.18	-9.86	-22.39	27.36	259271
-64.61	53	18.08	-6.34	13.68	4.49	22.83	-3.96	-15.52	19.83	207785
-64.23	51.93	19.75	-6.87	11.48	0.72	18.19	0.19	-8.68	12.15	176255
-62.62	50.87	21.3	-7.26	10.68	-0.3	18.43	1.01	-7.46	10.02	157403
-60.88	49.74	22.96	-7.65	11.45	0.1	19.08	1.18	-7.72	10	140608
-59.38	48.73	24.67	-8.06	13.25	1.21	17.74	1.74	-6.84	9.84	125001
-57.71	47.88	26.51	-8.49	14.56	2.15	15.48	2.5	-5.34	9.81	110697
-55.7	47.27	28.32	-8.91	15.12	2.63	13.86	2.88	-4.24	9.71	98003
-53.69	46.72	29.94	-9.29	15.27	2.67	13.66	2.59	-4.22	8.97	85336
-52.11	46.09	31.34	-9.6	14.94	2.88	14.28	2.33	-4.94	8.39	72434
-50.81	45.43	32.74	-9.92	14.09	3.07	14.95	1.98	-5.81	8.02	59120
-50.13	44.81	33.91	-10.29	13.01	5.11	22.21	0.59	-9.93	9.4	47087
-50.55	44.24	35.28	-10.78	13.27	11.89	46.27	-3.02	-20.99	13.77	37804
-52.34	43.56	36.84	-11.42	14.74	21.78	85.07	-7.73	-35.53	18.64	30818
-55.15	42.62	38.59	-12.23	15.86	27.4	115.41	-10.48	-42.81	19.79	26082
-57.89	41.34	40.51	-13.13	16.34	23.13	108.6	-9.87	-34.92	16.1	24323
-58.73	39.64	41.97	-13.79	16.97	14.04	69.27	-7.2	-16.4	9.8	22241
-58.21	37.89	43.88	-14.23	20.84	12.07	33.92	-7.78	-6.52	8.85	23407
-56.17	36.3	45.26	-14.38	28.59	21.89	34.01	-12.01	-10.89	12.77	28097
-53.48	34.9	46.51	-14.4	34.75	31.92	48.76	-14.78	-16.25	15.68	36025
-51.07	33.23	47.45	-14.34	37.66	37.81	59.44	-15.7	-18.56	16.34	38299
-48.8	31.48	48.63	-14.31	39.83	41.01	64.46	-14.94	-17.33	15.14	40877
-46.32	29.59	50.08	-14.28	44.69	47.37	72.81	-15.45	-17.31	14.57	45066

-43.99	27.65	51.63	-14.28	48.51	52.42	77.8	-16.09	-16.88	14.43	50276
-41.83	25.75	53.29	-14.31	51.12	56.48	81.81	-16.81	-17.11	14.95	56001
-39.86	23.87	54.95	-14.36	52.88	60.01	86.45	-17.65	-18.49	16.11	61553
-38.14	22.11	56.51	-14.44	54.12	62.63	91.78	-18.52	-20.88	17.26	66306
-36.49	20.47	57.97	-14.53	55.41	64.58	97.78	-19.01	-23.07	17.22	69208
-35.06	18.97	59.33	-14.65	55.62	65.15	103.02	-18.98	-24.55	16.48	68252
-33.66	17.5	60.68	-14.79	55.74	66.08	109.29	-19.34	-26.55	15.98	63535
-32.1	15.89	62.31	-14.97	55.22	66.2	115.59	-19.75	-29	15.58	55900
-30.71	14.36	63.48	-15.2	55.31	67.06	121.19	-20.22	-31.96	15.88	46858
-29.47	12.96	64.79	-15.49	55.98	69.68	125.64	-21.49	-34.94	16.94	37001
-27.79	11.31	65.8	-15.76	54.53	69.83	125.79	-21.98	-36.96	17.47	24619
-44.46	22.17	67	-18.76	836.99	101.46	20.82	-283.7	-34.98	106.42	32936
-39.89	18.39	69	-20.09	516.16	39.76	10.28	-144.9	-9.9	49.46	27173
-38.87	18.86	71.07	-20.56	385.03	2.88	3.52	-106.6	1.8	37.11	24391
-42.08	23.27	73.62	-19.96	385.44	13.47	5.32	-108.54	-0.67	37.18	23486
-44.41	25.71	75	-19.66	308.92	18.09	7.33	-82.85	-0.5	29.78	25160
-47.38	28.9	77	-19.48	249.09	13.89	7.77	-68.06	1.69	28.24	31050
-50.32	32.06	79.08	-19.46	308.56	14.31	6.82	-86.61	0.79	33.07	36201
-48.77	31.59	81	-20.13	271.9	6.22	3.91	-72.17	1.48	25.68	18372
-43.2	26.95	83	-21.78	137	2.08	2.05	-41.43	-0.16	19.02	2723

Figure 1. Hotspot chains on the African plate. Yellow stars represent hotspots used to constrain the model; other hotspots are shown as orange circles. Green triangles are locations of age dated seamounts. African plate boundaries are the Carlsberg Ridge (CR) denoting the India plate boundary, the Southwest Indian Ridge (SWIR) denoting the Antarctic plate boundary, and the Azores-Gibraltar Fracture Zone (AGFZ) between Africa and Eurasia. The Shaka Ridge (SR), Marion hotspot (MN), Crozet hotspot (CR), and Kerguelen hotspot (KU) are also labeled. Three sections of the plate are highlighted: the Southwest quadrant (A), Northwest quadrant (B), and the Eastern quadrant (C).

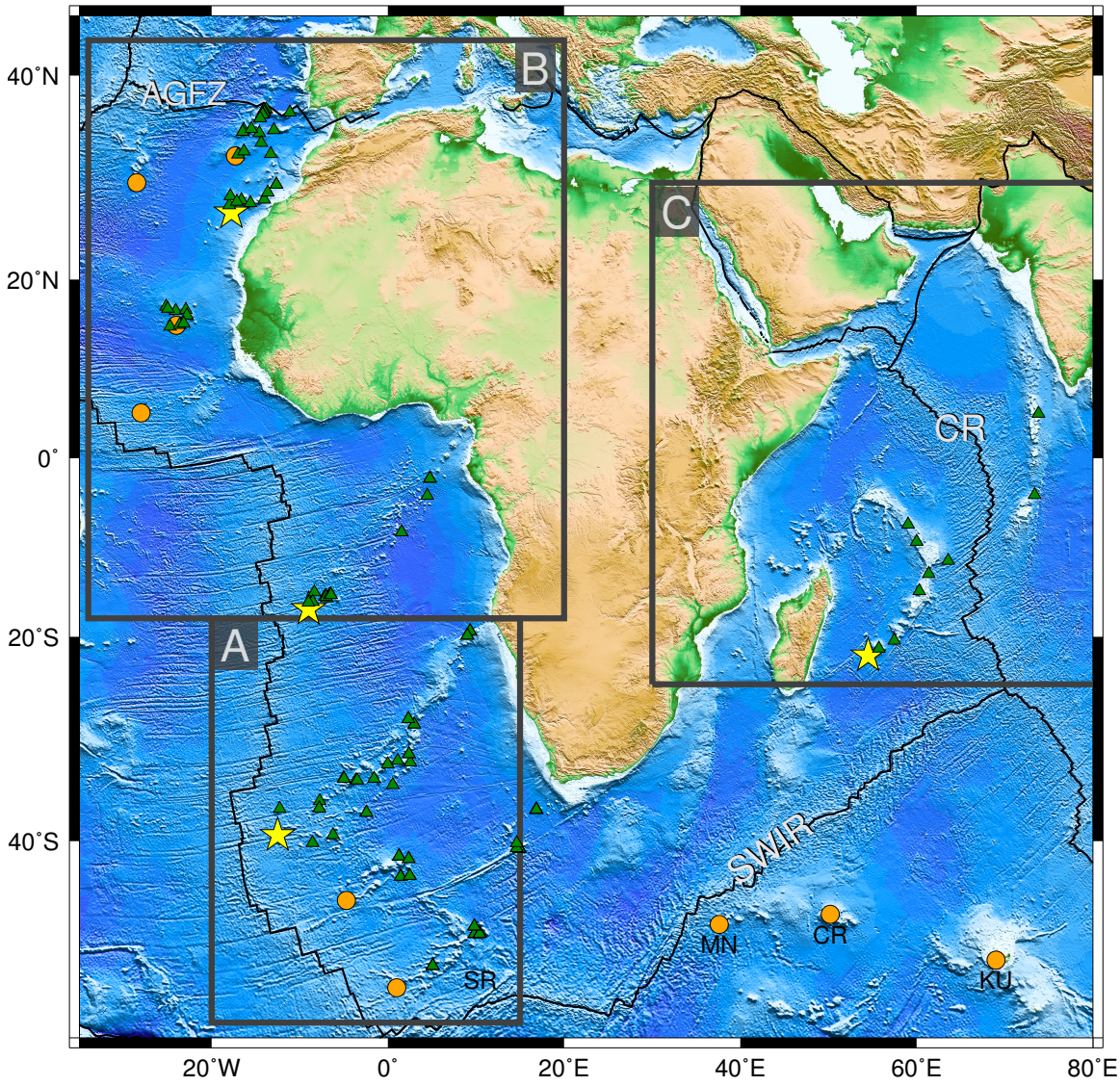

Figure 2. Hotspots in the southwest quadrant of the African plate. The Tristan (TR) hotspot chain, boxed in red with a yellow star showing the hotspot position, was used for modeling. The Discovery (DI) and Shona (SH) hotspots, shown in orange, were not. The purple diamond represents the location of Tristan da Cunha Island.

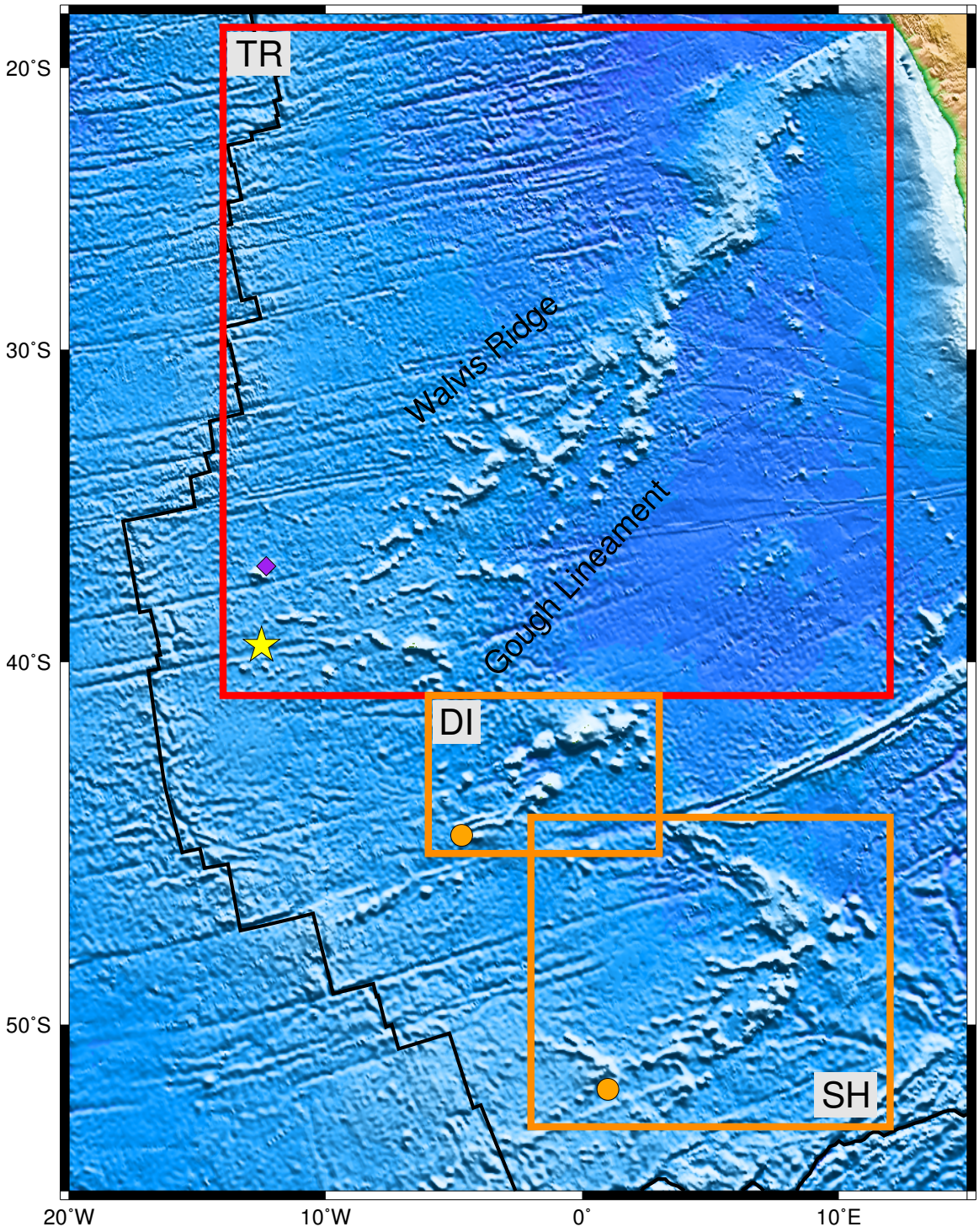

Figure 3. Previous models for the Tristan hotspot, with select observed ages as green triangles. Hotspot location for the O'Neill et al. (2005) model was stated to be Tristan da Cunha Island. Hotspot location for Duncan and Richards (1991) model was determined from Figure 3 in their paper. See legend for details.

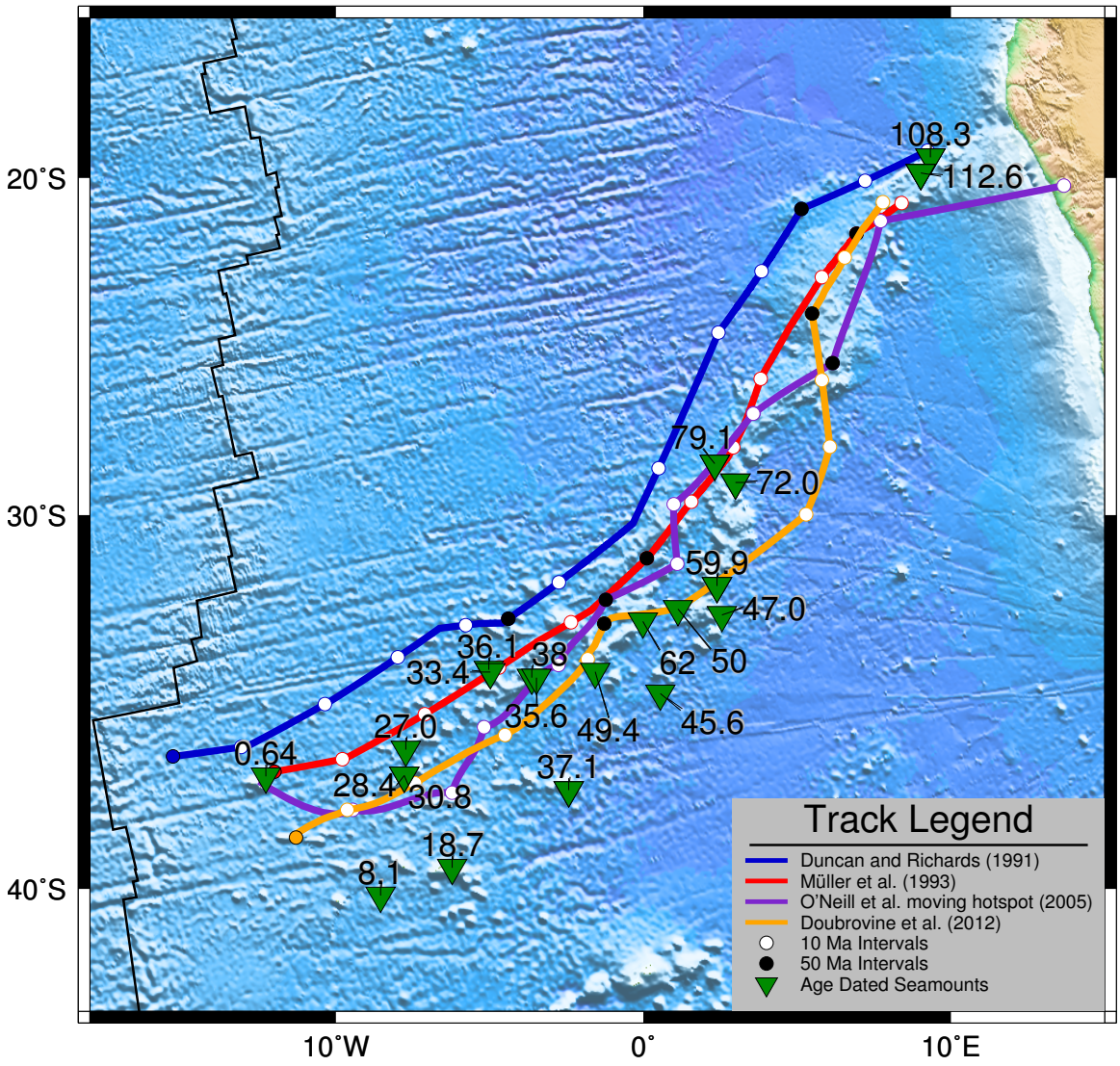

Figure 4. Previous models for the St. Helena hotspot with observed ages as green triangles. Hotspot location for Duncan and Richards (1991) model was determined from Figure 3 in their paper. Müller et al. (1993) hotspot location was chosen for best fit. See legend for details. The Cameroon Line (CL) overrides the oldest portion of the St. Helena chain in the north.

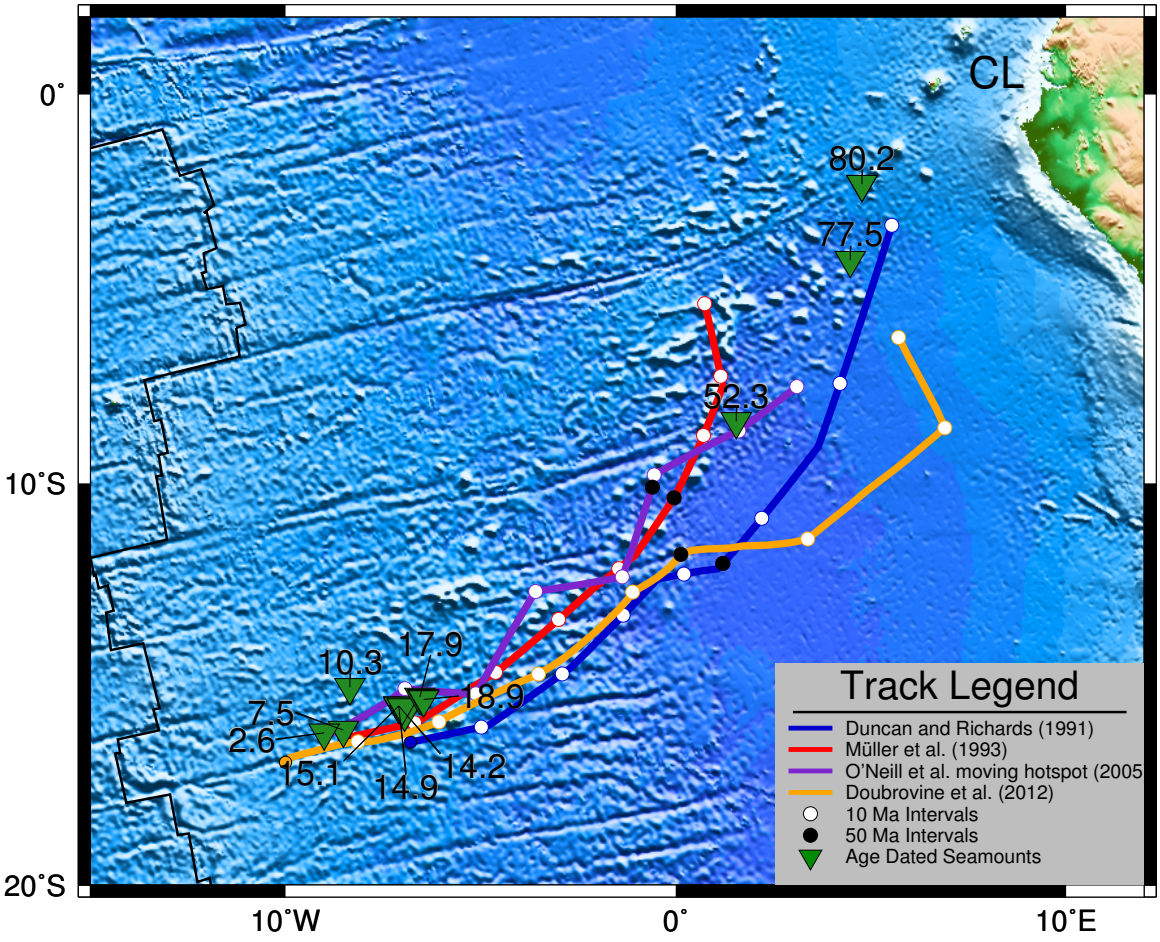

Figure 5. Hotspots in the northwest quadrant of the African plate. The Canary (CN) and St. Helena (ST) chains were used for modeling and shown in red boxes with yellow stars at the current hotspot positions. The Madeira (MA), Great Meteor (GM), Cape Verde (CV), and Bathymetrists (BA) hotspot chains are shown in orange boxes with orange circles at the hotspot positions. They were not used to create the model, but instead acted as checks for the resulting APM model. The Cameroon Line (CL), shown in the black box, is not considered a hotspot chain (Milelli et al., 2012). The location of the Carter Seamount is shown as a purple diamond.

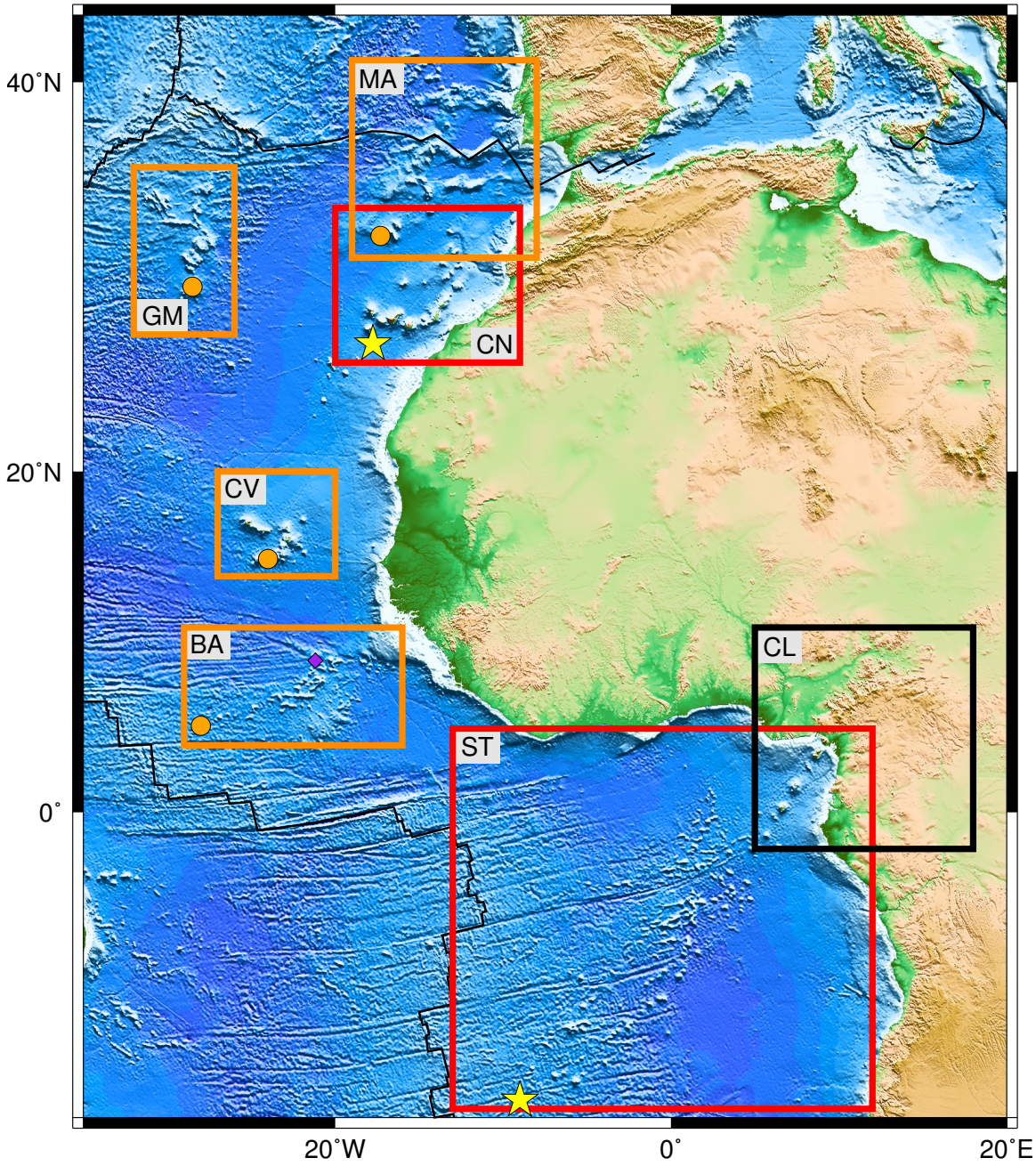

Figure 6. Previous models for the Canary hotspot with observed ages as green triangles, while Madeira age samples displaying Canary plume influence (Geldmacher et al., 2006) are shown as orange triangles. Hotspot location for Duncan and Richards (1991) model was determined from Figure 4 in their paper. Müller et al. (1993) hotspot location was chosen for best fit. O'Neill et al. (2005) did not include an estimate on Canary hotspot motion, so the fixed hotspot APM was used. Locations for Tenerife (T), La Palma (P), el Hierro (H), Fuerteventura (F), and Selvagem (S) Islands are shown. See legend for details.

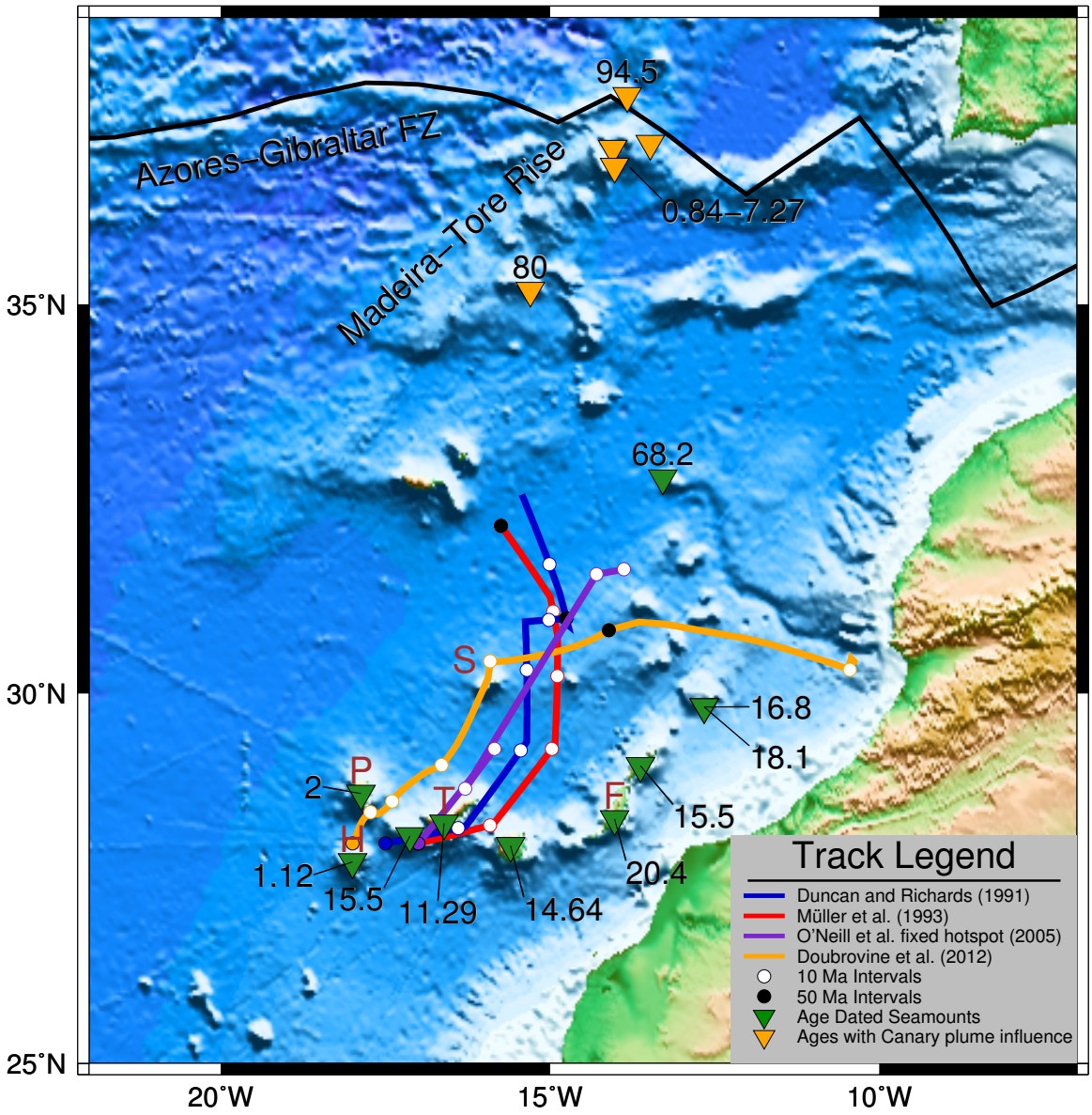

Figure 7. Hotspots on the eastern side of the African plate. The Réunion (RE) hotspot, boxed in red with a star indicating the hotspot position, was used for modeling. The Chagos-Laccadive Ridge (CH) was modeled using IND-AFR relative plate motions. The Comores (CO), in black, and the associated Farquhar atoll (F) was not considered a hotspot trail. The Deccan Traps, shown in purple, denotes the onset of the Réunion hotspot plume. The insert shows the location of key features on or near the Réunion hotspot track: the Seychelles microcontinent (S), Amirante Ridge (AR), Amirante Atolls (AA), Mascarene Plateau (MP), Saya de Malha Bank (SM), Nazareth Bank (N), Caragados Carajos Bank (C), Mauritius Island (M), Réunion Island (R), and the Rodriguez Ridge (RR).

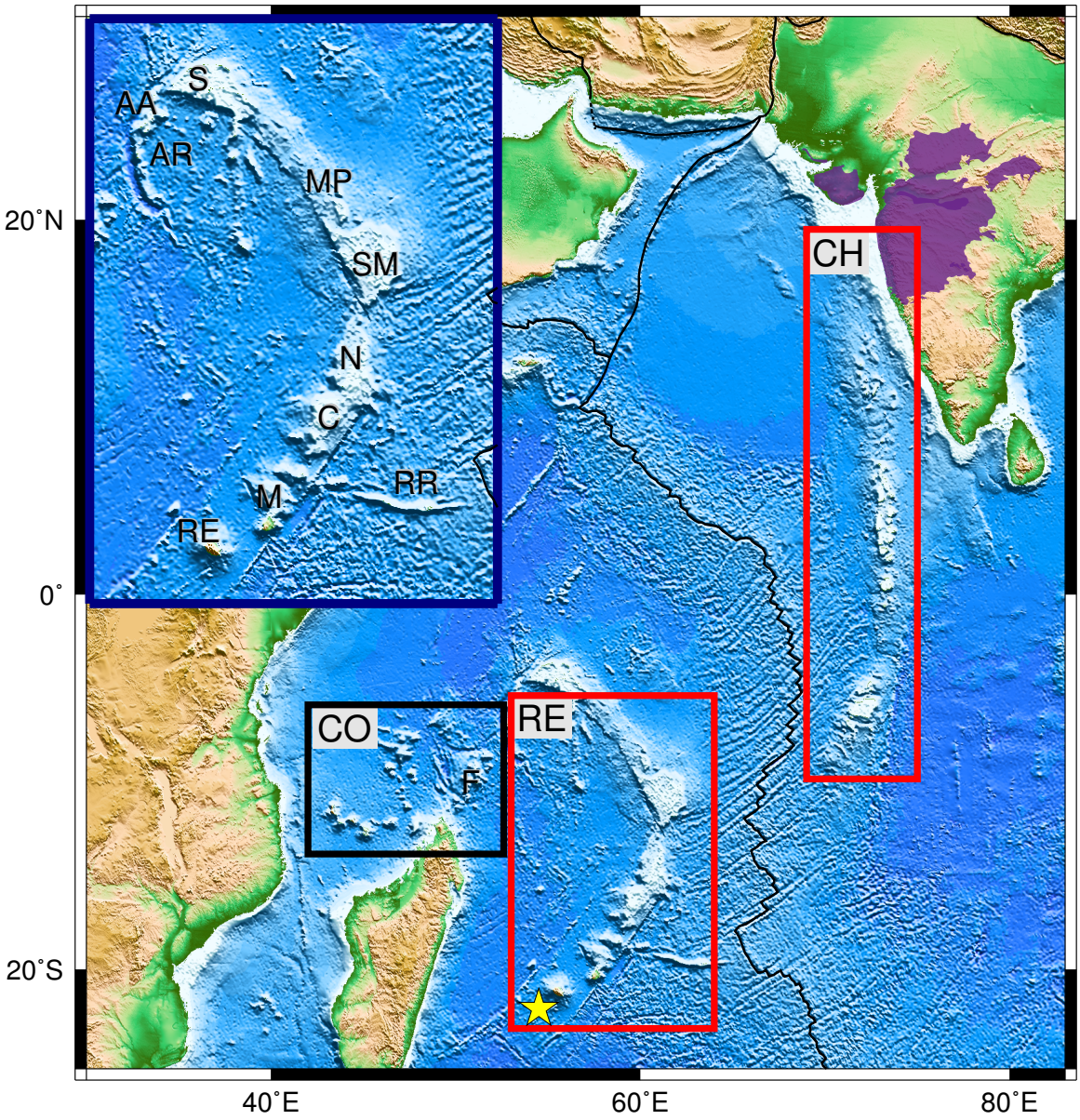

Figure 8. Previous models for the Réunion hotspot trail, with observed ages as green triangles. Duncan and Richards (1991) hotspot location estimated from Figure 5 in their paper. See legend for details.

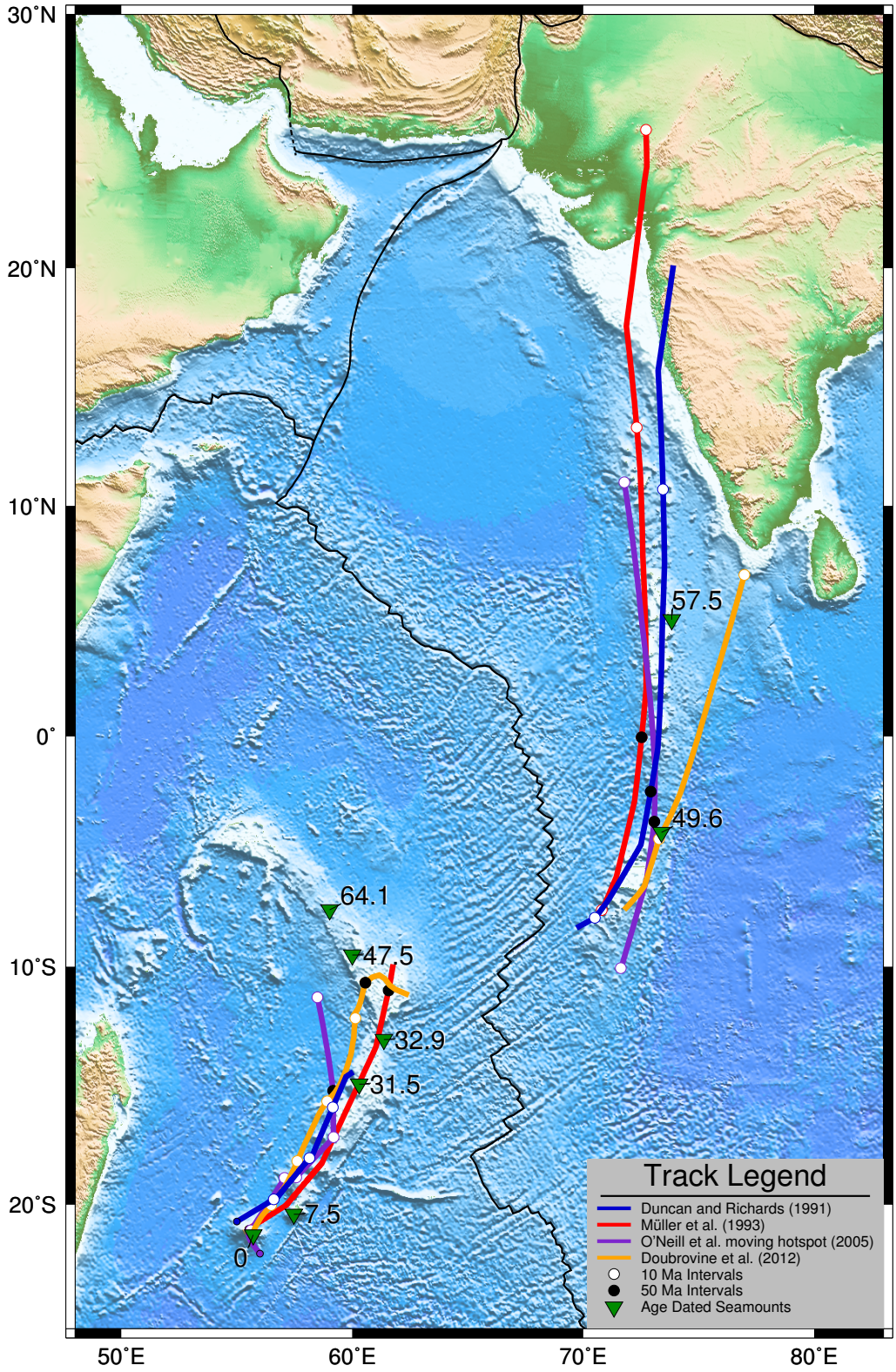

Figure 9. Stage A model for Canary (A), Réunion (B), and Tristan and St. Helena (C). Solid black lines are bisectors between hotspot location and a tentative "20 Ma" point shown as red circles. The resulting stage trail is shown as a red line. Oblique gridlines about the Euler pole (yellow star) are shown as dotted lines.

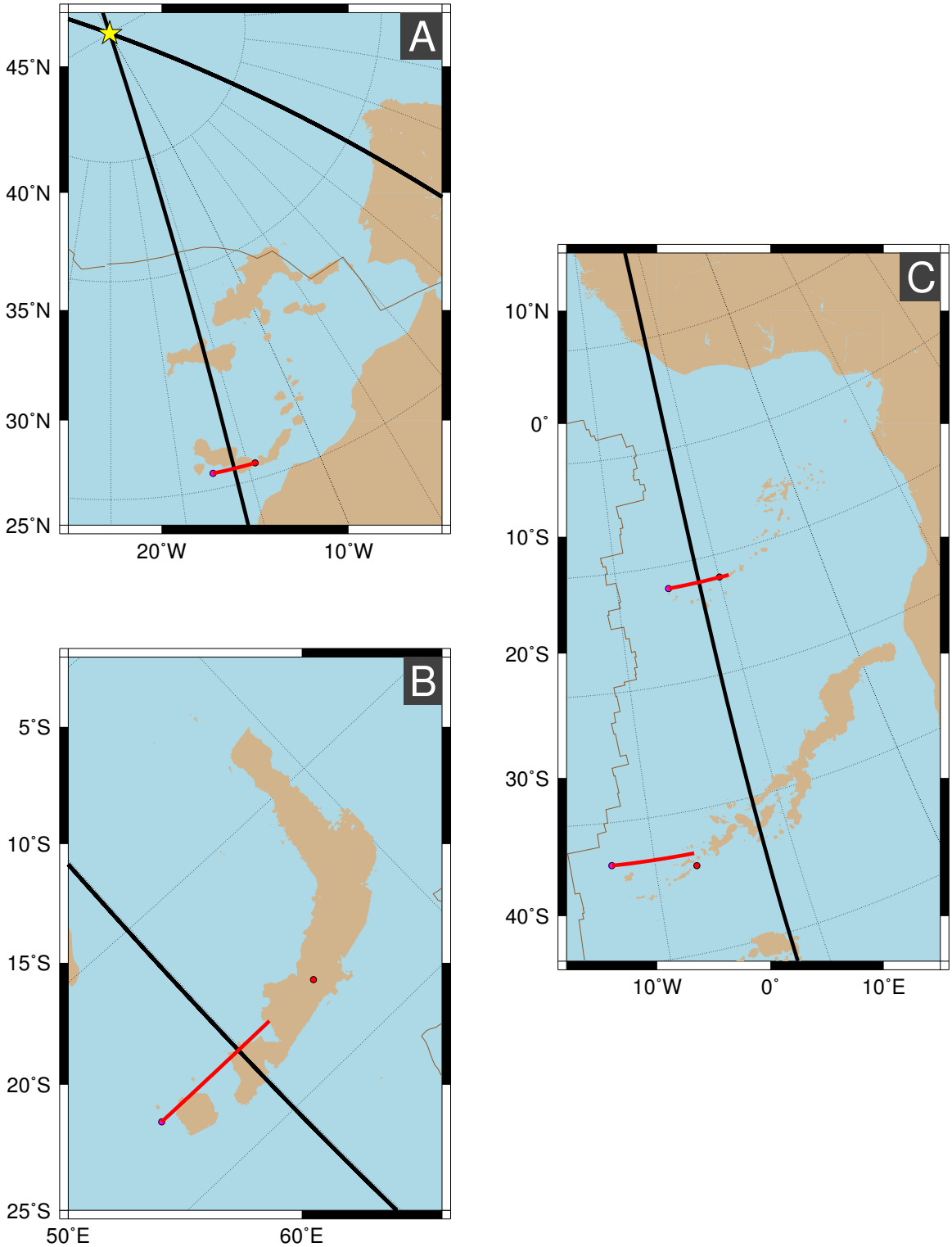

Figure 10. Magnetic anomaly picks between Africa and Antarctica that show a change in relative plate motion between Chron 21 and Chron 30. Reproduced from (Cande et al., 2010).

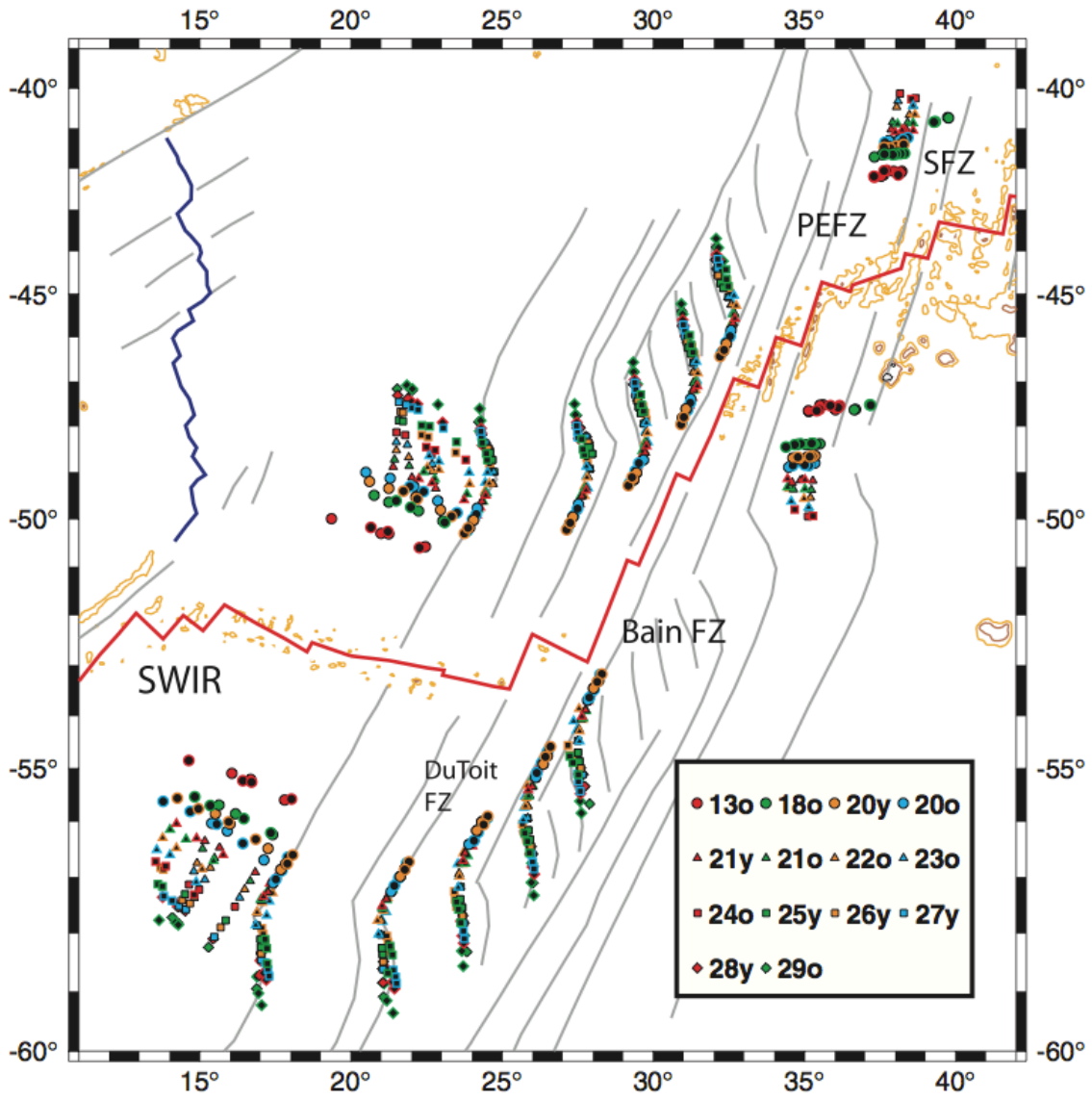

Figure 11. Stage B model for Canary (A), Réunion (B), and Tristan and St. Helena (C). The solid black line is the bisector between a tentative "20 Ma" point (red circle) and a "50 Ma" point (orange circle) on the Réunion hotspot track. A single-stage rotation pole was assumed to be located somewhere along its bisector. The resulting stage trail prediction for stage B is a red line, while previous stages are gray. Oblique gridlines about the Euler pole (yellow star) are shown as dotted lines.

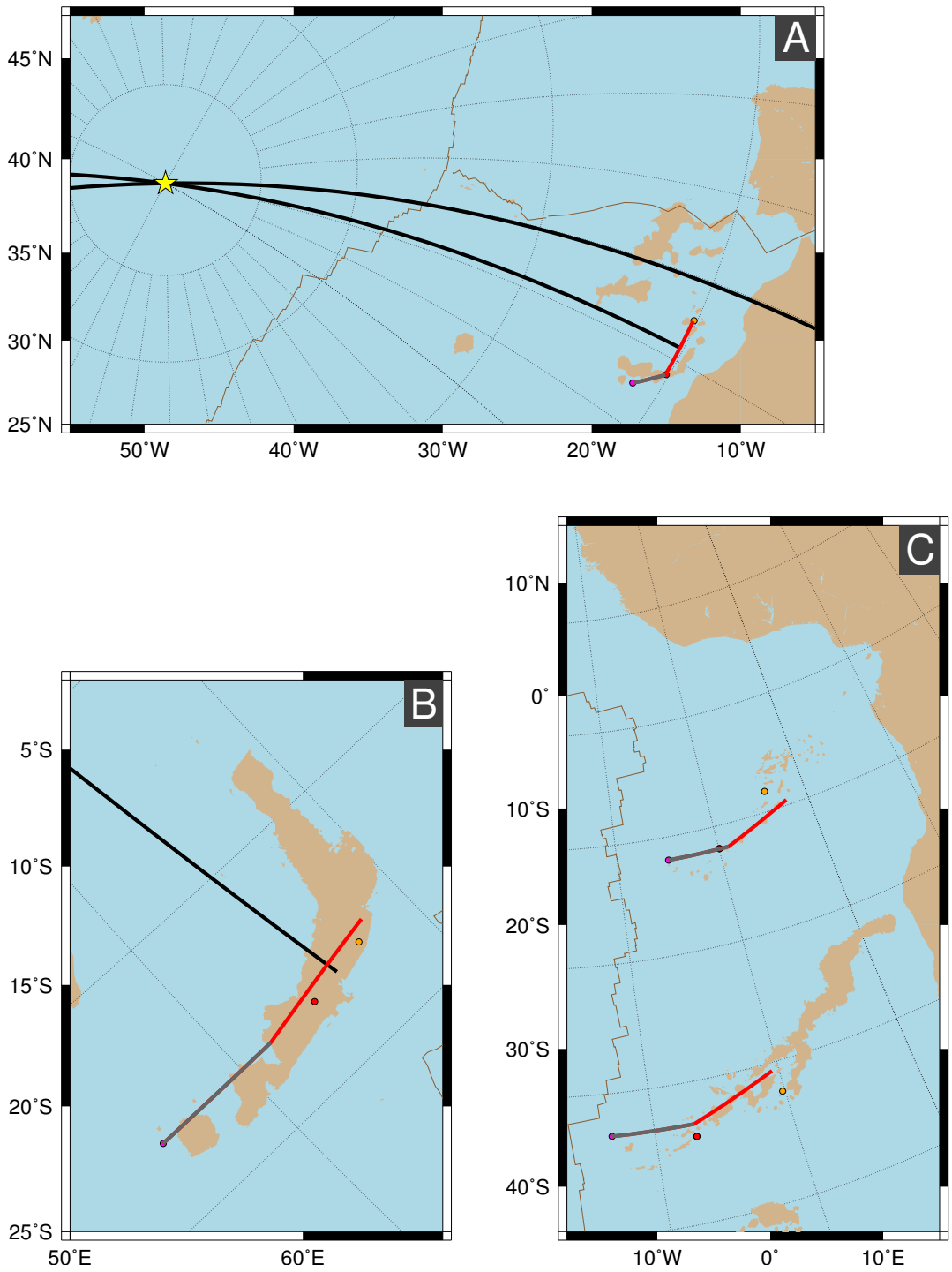

Figure 12. Stage C model for the Tristan chain. The solid black line is the bisector between a "50 Ma" point (orange circle) and a "67 Ma" point (yellow circle) on the Mascarene Plateau of the Réunion hotspot track. A single-stage rotation pole was assumed to be located somewhere along its bisector. If the rotation pole (yellow star) was to the west of the Tristan chain no reversal occurs along the hotspot track (A), but if a pole between Tristan and Africa was chosen the trail would experience a reversal along the Tristan chain (B). The resulting stage C rotation for each scenario is shown as a red line, while previous stages are gray. Oblique gridlines about the pole are shown as dotted lines.

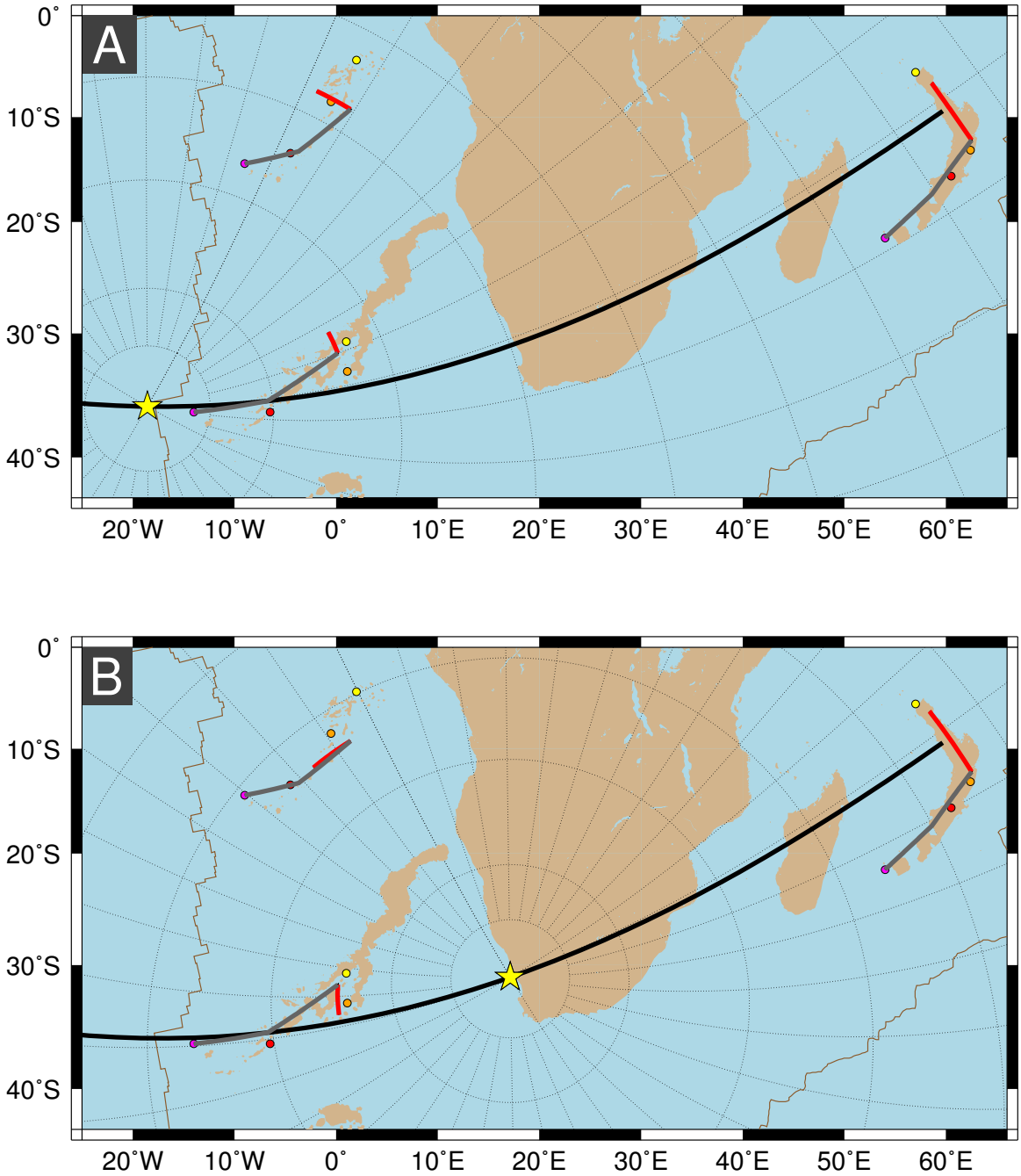

Figure 13. Stage D model for Tristan, Réunion and St. Helena chains, with a reversal (B) and without a reversal (A) inherited from stage C. The solid black lines are bisectors between a "67 Ma" point (yellow circle) and an "80" Ma point (white circle) on each of the Tristan and St. Helena chains. The resulting stage D trail prediction is shown as a red line, while previous stages are gray. Oblique gridlines about the pole (yellow star) are shown as dotted lines.

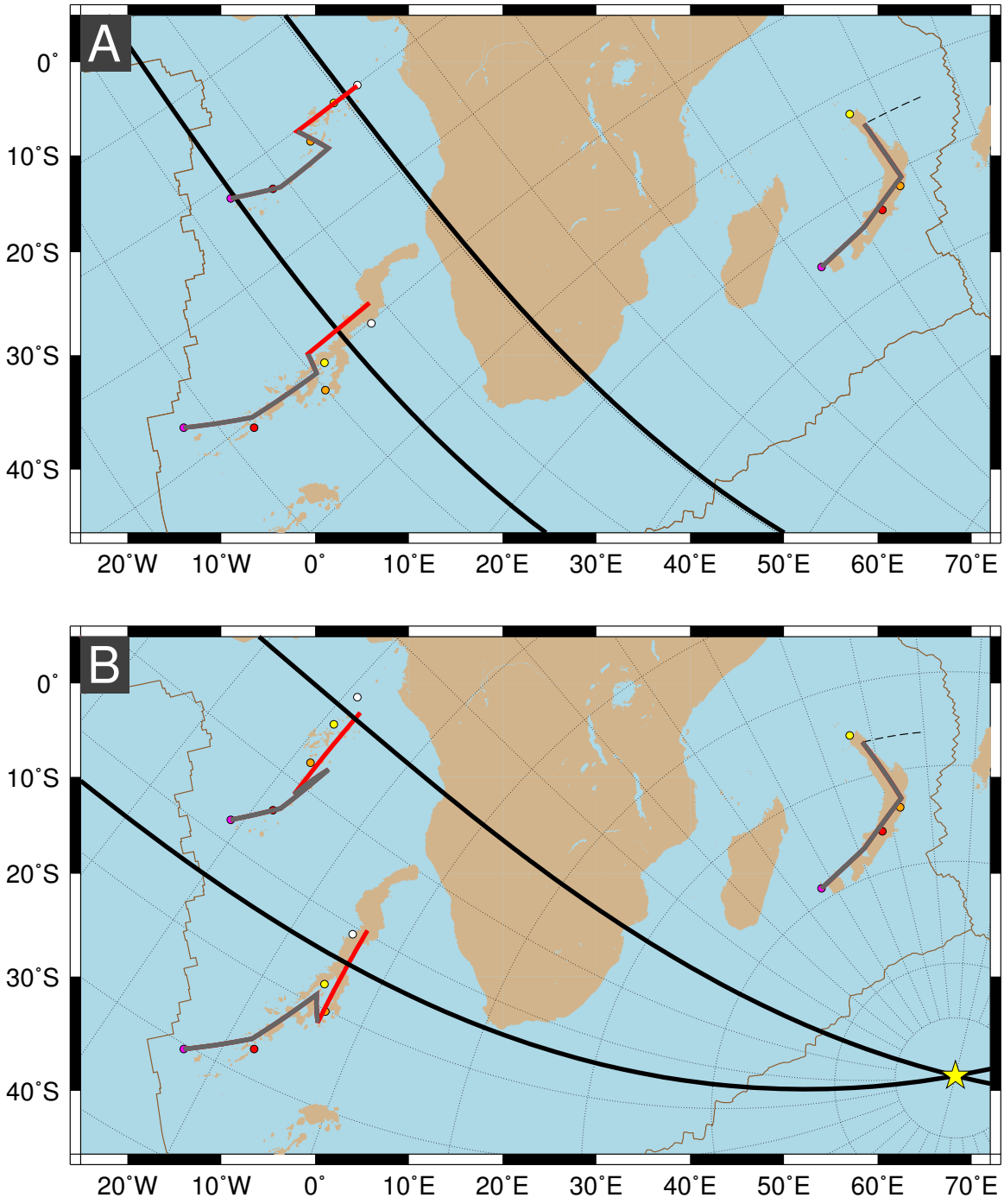

Figure 14. Residual topography of seamount chains. Envelopes for each chain are shown in gray, along with the elevation of the residual topography. A portion of the Chagos-Laccadive Ridge, the white polygon, was rotated back on the African plate (red line) using GPlates (version 1.2).

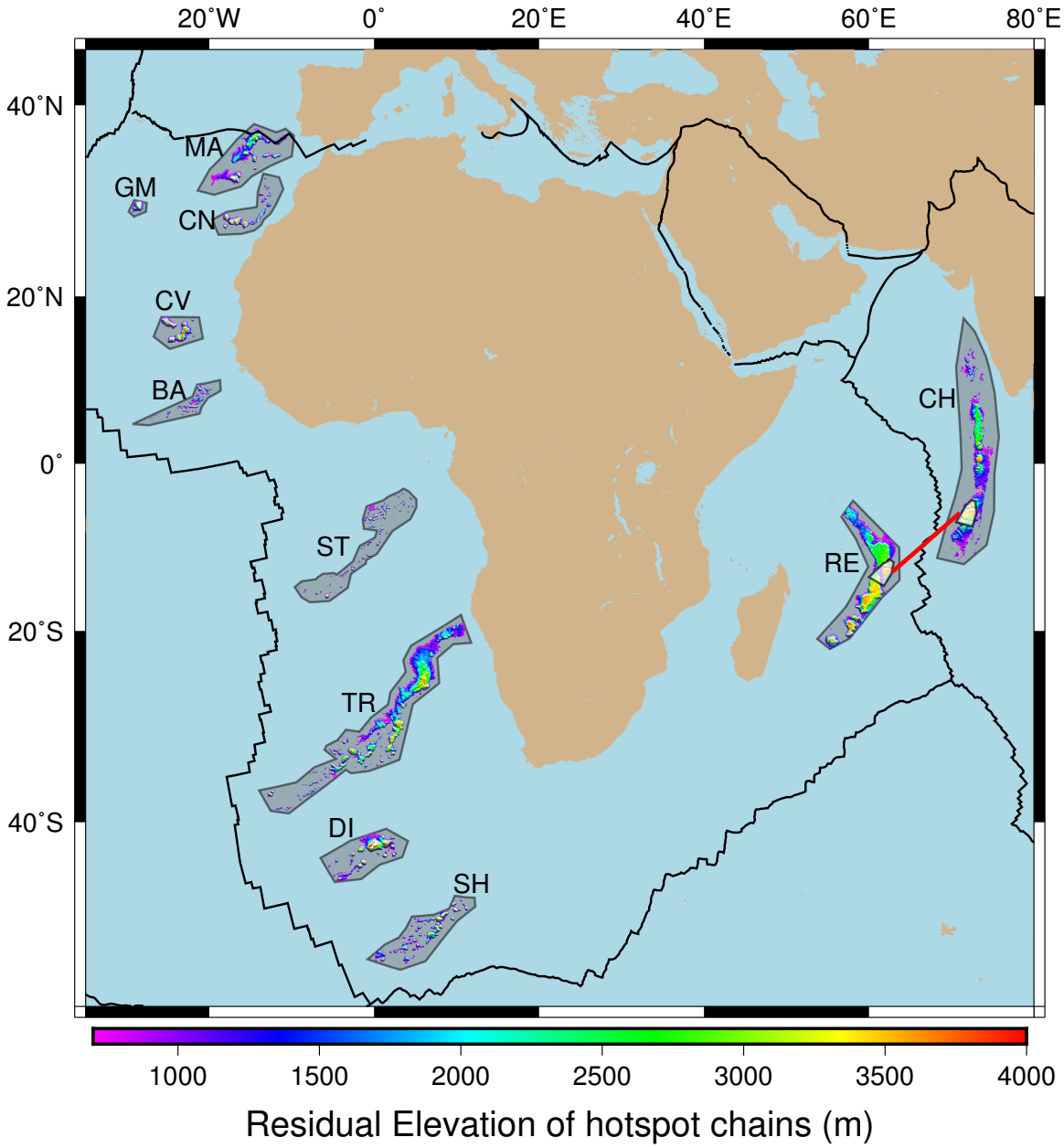

Figure 15. Revised Africa APM model. Select error ellipses are shown for simplicity. See Table 4 for the complete listing.

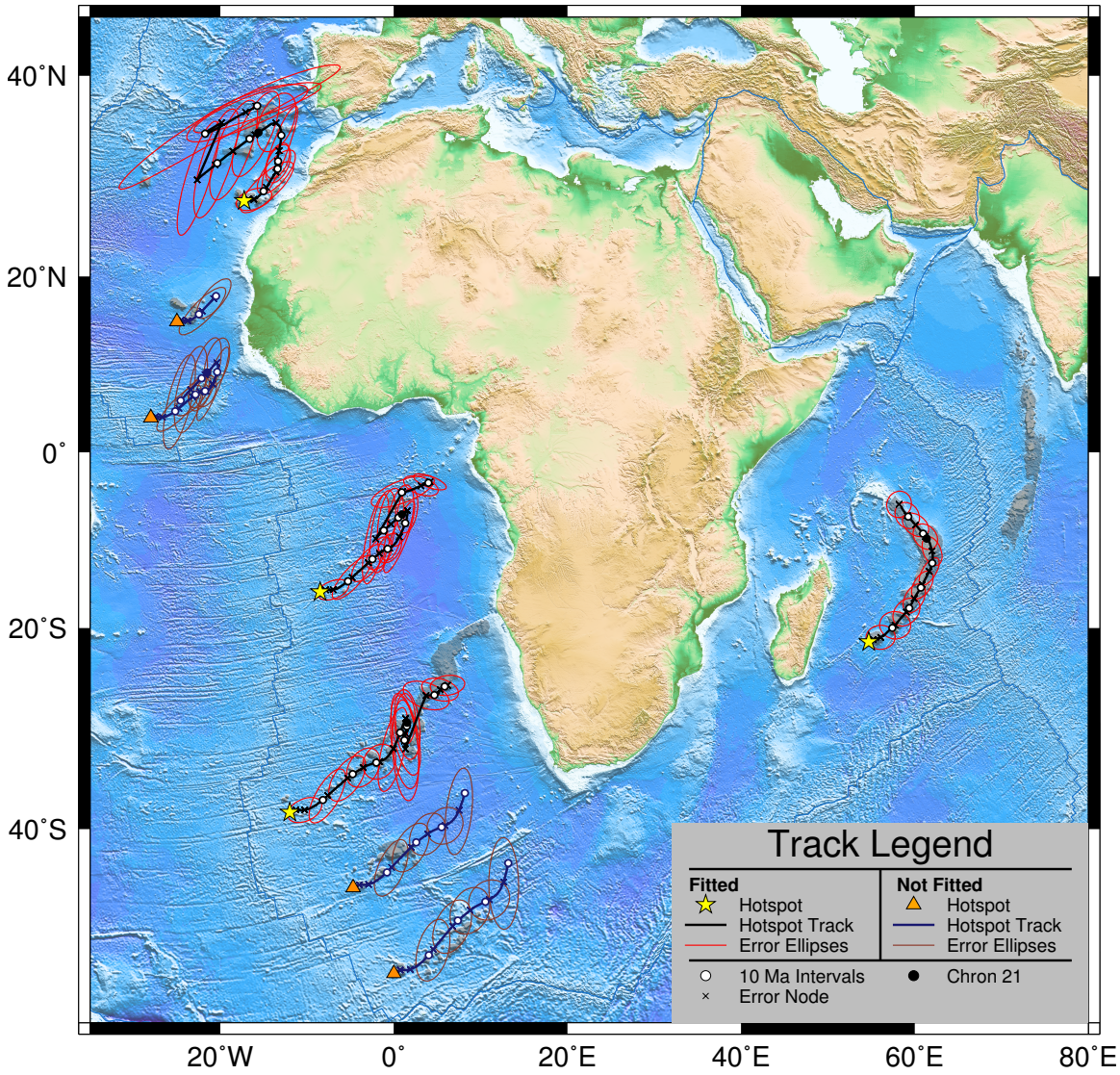

Figure 16. Africa APM predictions on the Chagos-Laccadive Ridge. The revised APM model has been reconstructed on the India plate using India-Africa RPMs from Seton et al. (2012), Cande et al. (2010), and Eagles and Hoang (2013).

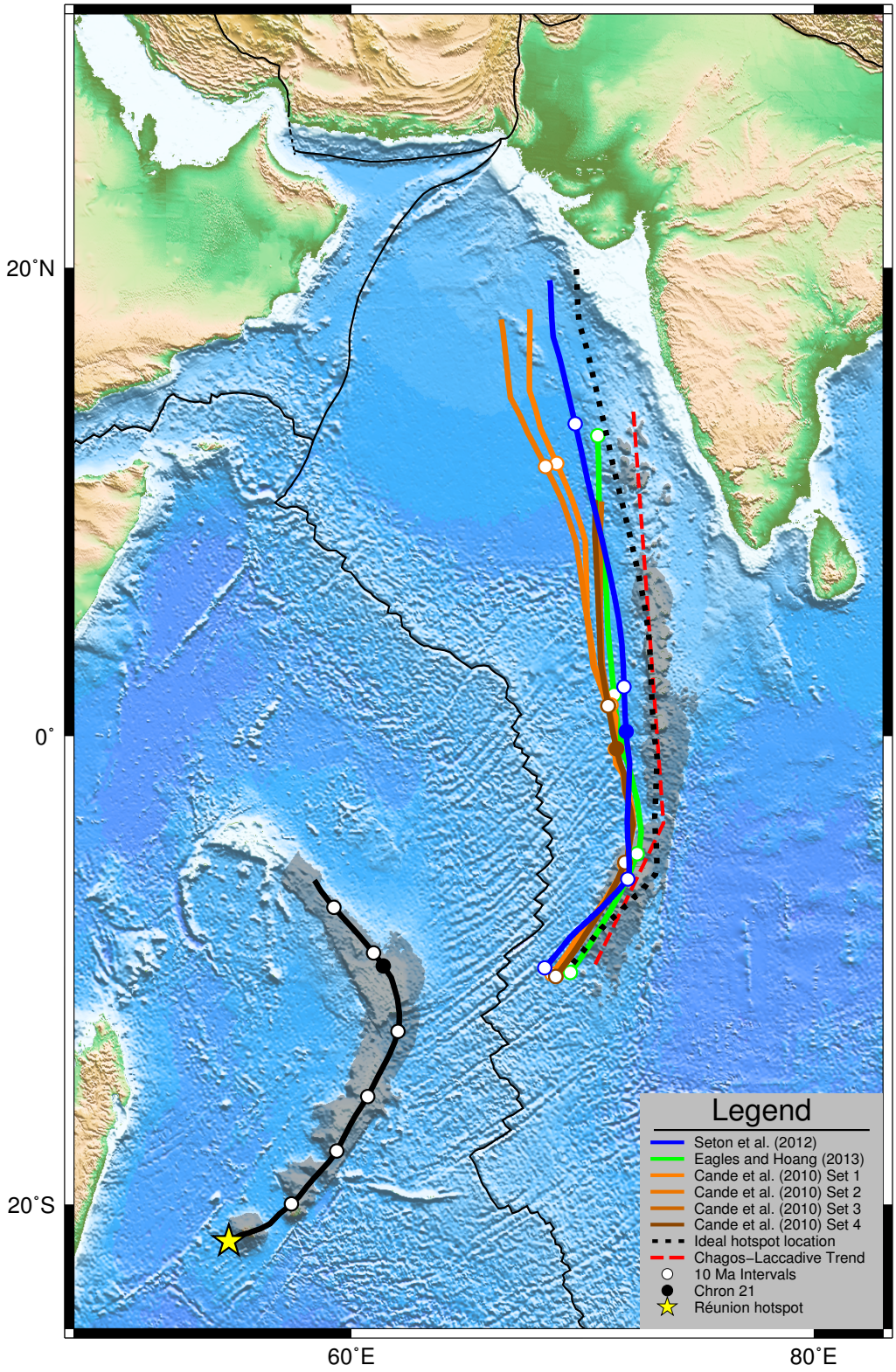

Figure 17. Finite and stage reconstruction poles of the revised APM model. Finite reconstruction poles are shown as circles along with uncertainties for ages older than 6 Ma. Earlier ages have too large of an uncertainty to display. Stage poles for 47–65 Ma are shown as triangles (inset).

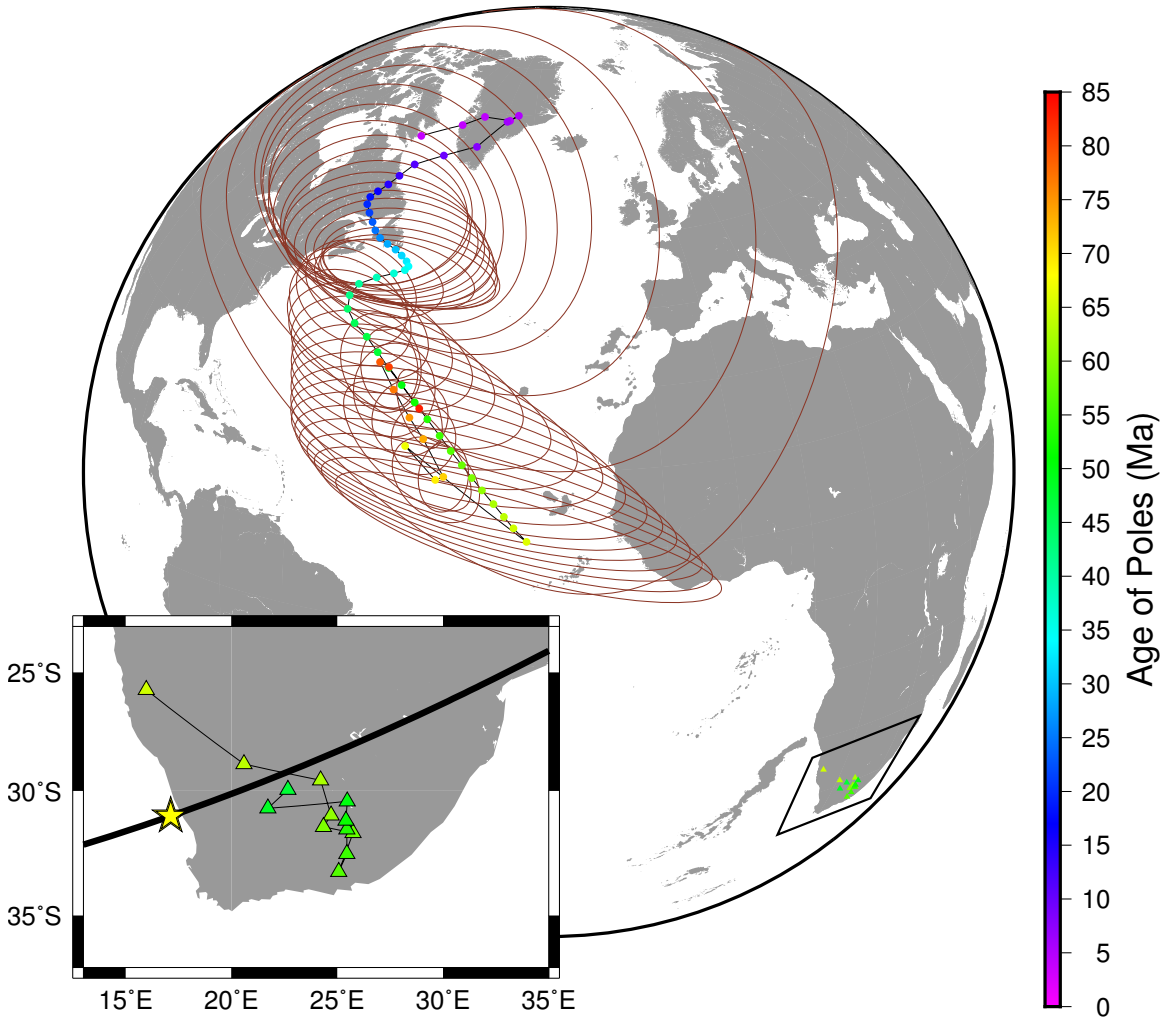

9. References

Ancochea, E., Hernán, F., Cendrero, A., Cantagrel, J. M., Fúster, J. M., Ibarrola, E., and Coello, J., 1994, Constructive and destructive episodes in the building of a young Oceanic Island, La Palma, Canary Islands, and genesis of the Caldera de Taburiente: J. Volcan. Geotherm. Res., v. 60, no. 3–4, p. 243–262.

Anderson, D. L., 2001, Top-Down Tectonics?: Science, v. 293, p. 2016–2018.

Backman, J., Duncan, R. A., and Party, S. S., 1988, Site 807: Proc. ODP Sci. Res., v. 115, no. 233–399.

Bernard, A., and Munschy, M., 2000, Were the Mascarene and Laxmi Basins (western Indian Ocean) formed at the same spreading centre?: Comptes Rendus de l'Academie des Sciences – Series IIA. Earth Planet. Sci., v. 330, no. 11, p. 777–783.

Bonneville, A., Barriot, J. P., and Bayer, R., 1988, Evidence from geoid data of a hotspot origin for the southern Mascarene Plateau and Mascarene Islands (Indian Ocean): J. Geophys. Res., v. 93, p. 4199-4212.

Breton, T., Nauret, F., Pichat, S., Moine, B., Moreira, M., Rose-Koga, E. F., Auclair, D., Bosq, C., and Wavrant, L.-M., 2013, Geochemical heterogeneities within the Crozet hotspot: Earth and Planetary Science Letters, v. 376, p. 126–136.

Bunce, E. T., and Chase, R. L., 1966, Preliminary results of the 1964 cruise of R.V. Chain to the Indian Ocean: Phil. Trans. R. Soc. Lond. A, v. 259, no. 1099, p. 218–226.

Burke, K. C., and Wilson, J. T., 1972, Is the Africa plate stationary?: Nature, v. 239, no. 5372, p. 387–389.

-, 1976, Hot spots on the Earth's surface: J. Geophys. Res., v. 93, p. 7690–7708.

Cande, S. C., Herron, E. M., and Hall, B. R., 1982, The Early Cenzoic tectonic history of the Southeast Pacific: Earth Planet. Sci. Lett., v. 57, p. 63–74.

Cande, S. C., Patriat, P., and Dyment, J., 2010, Motion between the Indian, Antarctic and African plates in the early Cenozoic: Geophys. J. Int., v. 183, p. 127–149.

Cande, S. C., and Stegman, D. R., 2011, Indian and African plate motions driven by the push force of the Réunion plume head: Nature, v. 475, p. 47–52.

Cantagrel, J. M., Cendrero, A., Fuster, J. M., Ibarrola, E., and Jamond, C., 1984, K-Ar chronology of the volcanic eruptions in the Canarian archipelago: Island of La Gomera: Bull. Volc., v. 47, no. 3, p. 597–609.

Caress, D. W., Menard, H. W., and Hey, R. N., 1988, Eocene reorganization of the Pacific-Farallon spreading center north of the Mendocino fracture zone: J. Geophys. Res., v. 93, no. B4, p. 2813–2838.

Chenet, A. L., Quidelleur, X., Fluteau, F., Courtillot, V., and Bajpai, S., 2007, 40K-40Ar dating of the Main Deccan large igneous province: Further evidence of KTB age and short duration: Earth and Planetary Science Letters, v. 263, no. 1-2, p. 1-15.

Coello, J., Cantagrel, J.-M., Hernán, F., Fúster, J.-M., Ibarrola, E., Ancochea, E., Casquet, C., Jamond, C., Díaz de Téran, J.-R., and Cendrero, A., 1992, Evolution of the eastern volcanic ridge of the Canary Islands based on new K–Ar data: J. Volcan. Geotherm. Res., v. 53, no. 1–4, p. 251–274.

Collier, J. S., Sansom, V., Ishizuka, O., Taylor, R. N., Minshull, T. A., and Whitmarsh, R. B., 2008, Age of Seychelles-India break-up: Earth and Planetary Science Letters, v. 272, p. 264–277.

Copley, A., Avouac, J.-P., and Royer, J. Y., 2010, India-Asia collision and the Cenozoic slowdown of the Indian plate: Implications for the forces driving plate motions: J. Geophys. Res., v. 115, no. B03410.

Courtillot, V., Davaille, A., Besse, J., and Stock, J., 2003, Three distinct types of hotspots in the Earth's mantle: Earth and Planetary Science Letters, v. 205, no. 3-4, p. 295-308.

Deppe, J., Hauff, F., Hoernle, K., Werner, R., Garge-Schönberg, D., O'Connor, J. M., and Jokat, W., 2010, Evidence for a long-term geochemical zonation of the Tristan-Gough Hotspot: Geophys. Res. Abstr., v. 12, p. EGU2010-4314.

Doubrovine, P. V., Steinberger, B., and Torsvik, T. H., 2012, Absolute plate motions in a reference frame defined by moving hot spots in the Pacific, Atlantic, and Indian oceans: J. Geophys. Res., v. 117, no. B9, p. B09101.

Duncan, R. A., and Hargraves, R. B., 1990, $^{40}Ar/^{39}Ar$ Geochronology of basement rocks from the Mascarene Plateau, the Chagos Bank, and the Maldives Ridge: Proc. ODP Sci. Res., v. 115, p. 43–51.

Duncan, R. A., and Richards, M. A., 1991, Hotspots, mantle plumes, flood basalts, and true polar wander: Rev. Geophys., v. 29, no. 1, p. 31–50.

Eagles, G., and Hoang, H. H., 2013, Cretaceous to present kinematics of the Indian, African and Seychelles plates: Geophys. J. Int.

Emerick, C. M., and Duncan, R. A., 1982, Age progressive volcanism in the Comores Archipelago, western Indian Ocean and implications for Somali plate tectonics: Earth and Planetary Science Letters, v. 60, p. 415–428.

Fisher, R. L., Johnson, G. L., and Heezen, B. C., 1967, Mascarene Plateau, western Indian Ocean: Geol. Soc. Am. Bull., v. 78, p. 1247–1266.

Ganerød, M., Torsvik, T. H., Van Hinsbergen, D. J. J., Gaina, C., Corfu, F., Werner, S., Owen-Smith, T. M., Ashwal, L. D., Webb, S. J., and Hendriks, B. W. H., 2011, Paleoposition of the Seychelles microcontinent in relation to the Deccan Traps and the plume generation zone in Late Cretaceous–Early Palaeogene time, *in* Van Hinsbergen, D. J. J., Buiter, S. J. H., Torsvik, T. H., Gaina, C., and Webb, S. J., eds., The Formation and Evolution of Africa: A Synopsis of 3.8 Ga of Earth History, Volume 357: Geol. Soc. Lond. Spec. Publ., The Geological Society of London, p. 229–252.

Geldmacher, J., Hoernle, K., Bogaard, P. v. d., Duggen, S., and Werner, R., 2005, New 40Ar / 39Ar age and geochemical data from seamounts in the Canary and Madeira volcanic provinces: Support for the mantle plume hypothesis: Earth and Planetary Science Letters, v. 237, no. 1-2, p. 85.

Geldmacher, J., Hoernle, K., Klügel, A., Bogaard, P. v. d., Wombacher, F., and Berning, B., 2006, Origin and geochemical evolution of the Madeira-Tore Rise (eastern north Atlantic): J. Geophys. Res., v. 111, no. B09206.

Geldmacher, J., Hoernle, K., van den Bogaard, P., Zankl, G., and Garbe-Schonberg, D., 2001, Earlier history of the ≥70-Ma-old Canary hotspot based on the temporal and geochemical evolution of the Selvagen Archipelago and neighboring seamounts in the eastern North Atlantic: J. Volcan. Geotherm. Res., v. 111, p. 55–87.

Guillou, H., Carracedo, J. C., Torrado, F. P., and Badiola, E. R., 1996, K-Ar ages and magnetic stratigraphy of a hotspot-induced, fast grown oceanic island: El Hierro, Canary Islands: J. Volcan. Geotherm. Res., v. 73, no. 1–2, p. 141–155.

Guillou, H., Torrado, F. J. P., Hansen Machin, A. R., Carracedo, J. C., and Gimeno, D., 2004, The Plio–Quaternary volcanic evolution of Gran Canaria based on new K–Ar ages and magnetostratigraphy: J. Volcan. Geotherm. Res., v. 135, no. 3, p. 221–246.

Hall, S., and Bird, D., 2007, Tristan da Cuhna hotspot tracks and the seafloor spreading history of the South Atlantic: Eos Trans. AGU, v. 88, p. V31F-04.

Holm, P. M., Grandvuinet, T., Friis, J., Wilson, J. R., Barker, A. K., and Plesner, S., 2008, An 40Ar-39Ar study of the Cape Verde hot spot: Temporal evolution in a semistationary plate environment: J. Geophys. Res., v. 113, no. B0820, p. doi:10.1029/2007JB005339.

Koppers, A. A. P., Yamazaki, T., Geldmacher, J., Gee, J. S., Pressling, N., Koppers, A. A. P., Yamazaki, T., Geldmacher, J., Gee, J. S., Pressling, N., Hoshi, H., Anderson, L., Beier, C., Buchs, D. M., Chen, L. H., Cohen, B. E., Deschamps, F., Dorais, M. J., Ebuna, D., Ehmann, S., Fitton, J. G., Fulton, P. M., Ganbat, E., Hamelin, C., Hanyu, T., Kalnins, L., Kell, J., Machida, S., Mahoney, J. J., Moriya, K., Nichols, A. R. L., Rausch, S., Sano, S. i., Sylvan, J. B., and Williams, R., 2012, Limited latitudinal mantle plume motion for the Louisville hotspot: Nature Geosci, v. 5, no. 10.1038/ngeo1638.

McDougall, I., 1971, The geochronology and evolution of the young volcanic island of Réunion, Indian Ocean: Geochimica et Cosmochimica Acta, v. 35, p. 261–288.

McNutt, M. K., 1988, Thermal and mechanical properties of the Cape Verde Rise: J. Geophys. Res., v. 93, no. B4, p. 2784–2794.

Meyerhoff, A. A., and Kamen-Kaye, M., 1981, Petroleum prospects of Saya de Malha and Nazareth Banks, Indian Ocean: AAPG Bull., v. 65, no. 1344–1347.

Milelli, L., Fourel, L., and Jaupart, C., 2012, A lithospheric instability origin for the Cameroon Volcanic Line: Earth and Planetary Science Letters, v. 235–236, p. 80–87.

Molnar, P., and Stock, J., 1987, Relative motions of hotspots in the Pacific, Atlantic and Indian Oceans since Late Cretaceous time: Nature, v. 327, p. 587–591.

Morgan, J. W., 1981, Hotspot tracks and the opening of the Atlantic and Indian oceans, *in* Emiliani, C., ed., The sea, Volume 7: New York, Wiley.

Morra, G., Seton, M., Quevedo, L., and Müller, R. D., 2013, Organization of the tectonic plates in the last 200Myr: Earth and Planetary Science Letters, v. 373, no. 0, p. 93-101.

Müller, R. D., Royer, J.-Y., and Lawver, L. A., 1993, Revised plate motions relative to the hotspots from combined Atlantic and Indian Ocean hotspot tracks: Geology, v. 21, no. 3, p. 275–278.

Müller, R. D., Royer, J. Y., Cande, S. C., Roest, W. R., and Maschenkov, S., 1999, New constraints on Carribean plate tectonic evolution, *in* Mann, P., ed., Caribbean basins: Amsterdam, Elsevier, p. 39–55.

Müller, R. D., Sdrolias, M., Gaina, C., and Roest, W. R., 2008, Age, spreading rates, and spreading asymmetry of the world's ocean crust: Geochem. Geophys. Geosyst., v. 9, no. Q04006, p. doi:10.1029/2007GC001743.

O'Connor, J. M., and Duncan, R. A., 1990, Evolution of the Walvis Ridge-Rio Grande Rise hot spot system: Implications for African and South American plate motions of plumes: J. Geophys. Res., v. 95, p. 17,475–417,502.

O'Connor, J. M., Jokat, W., le Roex, A. P., Class, C., Wijbrans, J. R., Keßling, S., Kuiper, K. F., and Nebel, O., 2012, Hotspot trails in the South Atlantic controlled by plume and plate tectonic processes: Nature Geoscience, v. 5, p. 735–738.

O'Connor, J. M., and Le Roex, A. P., 1992, South Atlantic hot spot-plume systems: 1. Distribution of volcanism in time and space: Earth and Planetary Science Letters, v. 113, no. 3, p. 343–364.

O'Connor, J. M., Steinberger, B., Regelous, M., Koppers, A. A., Wijbrans, J. R., Haase, K. M., Stoffers, P., Jokat, W., and Garbe-Schonberg, D., 2013, Constraints on past plate and mantle motion from new ages for the Hawaiian-Emperor Seamount Chain: Geochem. Geophys. Geosyst.

O'Connor, J. M., Stoffers, P., van den Bogaard, P., and McWilliams, M., 1999, First seamount age evidence for significantly slower African plate motion since 19 to 30 Ma: Earth and Planetary Science Letters, v. 171, no. 4, p. 575-589.

O'Neill, C., Müller, D., and Steinberger, B., 2005, On the uncertainties in hot spot reconstructions and the significance of moving hot spot reference frames: Geochem. Geophys. Geosyst., v. 6, no. 4, p. Q04003.

Rohde, J. K., van den Bogaard, P., Hoernle, K., Hauff, F., and Werner, R., 2013, Evidence for an age progression along the Tristan-Gough volcanic track from new $^{40}Ar/^{39}Ar$ ages on phenocryst phases: Tectonophysics, v. 604, p. 60–71.

Royer, J. Y., Gordon, R. G., and Horner-Johnson, B. C., 2006, Motion of Nubia relative to Antarctica since 11 Ma: Implications for Nubia-Somalia, Pacific-North America, and India-Eurasia motion: Geology, v. 34, p. 501–504.

Sager, W. W., and Tominaga, M., 2008, Paleomagnetism of Basaltic Rocks Cored from the Walvis Ridge, South Atlantic and Implications for Hotspot Paleolatitude: Eos Trans. AGU, v. 89, no. Fall Meeting p. Abstract GP14A-05.

Seton, M., Müller, R. D., Zahirovic, S., Gaina, C., Torsvik, T., Shephard, G. E., Talsma, A. S., Gurnis, M., Turner, M., Maus, S., and Chandler, M. T., 2012, Global continental and ocean basin reconstructions since 200 Ma: Earth Science Reviews, v. 113, p. 212–270.

Sharp, W. D., and Clague, D. A., 2006, 50-Ma initiation of Hawaii-Emperor bend records major change in Pacific plate motion: Science, v. 313, p. 1281–1284.

Skolotnev, S. G., Bel'tenev, V. E., Lepekhina, E. N., and Ipat'eva, I. S., 2010, Younger and Older Zircons from Rocks of the Oceanic Lithosphere in the Central Atlantic and Their Geotectonic Implications: Geotectonics, v. 44, no. 6, p. 462–492.

Steinberger, B., Sutherland, R., and O'Connell, R. J., 2004, Prediction of Emperor-Hawaii seamount locations from a revised model of global plate motion and mantle flow: Nature, v. 430, p. 167–173.

Tarduno, J. A., Duncan, R. A., Scholl, D. W., Cottrell, R. D., Steinberger, B., Thordarson, T., Kerr, B. C., Neal, C. R., Frey, F. A., Torii, M., and Carvallo, C., 2003, The Emperor Seamounts: Southward Motion of the Hawaiian Hotspot Plume in Earth's Mantle: Science, v. 301, no. 5636, p. 1064-1069.

Thirlwall, M. F., Singer, B. S., and Marriner, G. F., 2000, ^{39}Ar–^{40}Ar ages and geochemistry of the basaltic shield stage of Tenerife, Canary Islands, Spain: J. Volcan. Geotherm. Res., v. 103, p. 247–297.

Torsvik, T., Müller, R. D., Van der Voo, R., Steinberger, B., and Gaina, C., 2008, Global Plate Motion Frames: Toward a unified model: Rev. Geophys., v. 46, no. RG3004.

Torsvik, T., Tucker, R. D., Ashwal, L. D., Eide, E. A., Rakotosolofo, N. A., and de Wit, M. J., 1998, Late Cretaceous magmatism in Madagascar: Palaeomagnetic evidence for a stationary Marion hotspot: Earth and Planetary Science Letters, v. 164, p. 221–232.

Torsvik, T. H., Amundsen, H., Hartz, E. H., Corfu, F., Kusznir, N., Gaina, C., Doubrovine, P. V., Steinberger, B., Ashwal, L. D., and Jamtveit, B., 2013, A Precambrian microcontinent in the Indian Ocean: Nature Geosci, v. 6, p. 223–227.

Tucholke, B. E., and Smoot, N. C., 1990, Evidence for age and evolution of Corner seamounts and Great Meteor seamount chain from multibeam bathymetry: J. Geophys. Res., v. 95, no. B11, p. 17,555–517,569.

Vandamme, D., and Courtillot, V., 1990, Latitudinal evolution of the Réunion hotpsot deduced from paleomagnetic results of Leg 115: Geophys. Res. Lett., v. 17, no. 8, p. 1105–1108.

Wessel, P., Harada, Y., and Kroenke, L. W., 2006, Towards a self-consistent, high-resolution absolute plate motion model for the Pacific: Geochem. Geophys. Geosyst., v. 7, no. Q03L12.

Wessel, P., and Kroenke, L. W., 2008, Pacific absolute plate motions since 145 Ma: An assessment of the fixed hotspot hypothesis: J. Geophys. Res., v. 113, no. B06101, p. doi:10.1029/2007JB005499.

Wessel, P., and Kroenke, L. W., 2009, Observations of geometry and ages constrain relative motion of Hawaii and Louisville plumes: Earth and Planetary Science Letters, v. 284, no. 3/4, p. 467–472.

Whittaker, J. M., Muller, R. D., Leitchenkov, G., Stagg, H., Sdrolias, M., Gaina, C., and Goncharov, A., 2007, Major Australian-Antarctic Plate Reorganization at Hawaiian-Emperor Bend Time: Science, v. 318, no. 5847, p. 83–86.

Whittaker, J. M., Williams, S. E., and Müller, R. D., 2013, Revised tectonic evolution of the Eastern Indian Ocean: Geochemistry, Geophysics, Geosystems, v. 14, no. 6, p. 1891-1909.